NASA TECHNICAL NOTE **NASA TN D-2214**

NASA TN D-2214

EXPERIMENTAL LATERAL VIBRATION CHARACTERISTICS OF A 1/5-SCALE MODEL OF SATURN SA-1 WITH AN EIGHT-CABLE SUSPENSION SYSTEM

by John S. Mixson and John J. Catherine

Langley Research Center

Langley Station, Hampton, Va.

NATIONAL AERONAUTICS AND SPACE ADMINISTRATION • WASHINGTON, D. C. • NOVEMBER 1964

EXPERIMENTAL LATERAL VIBRATION CHARACTERISTICS OF A 1/5-SCALE MODEL OF SATURN SA-1 WITH AN EIGHT-CABLE SUSPENSION SYSTEM

By John S. Mixson and John J. Catherine

Langley Research Center
Langley Station, Hampton, Va.

NATIONAL AERONAUTICS AND SPACE ADMINISTRATION

For sale by the Office of Technical Services, Department of Commerce,
Washington, D.C. 20230 -- Price $1.50

EXPERIMENTAL LATERAL VIBRATION CHARACTERISTICS OF A 1/5-SCALE MODEL OF SATURN SA-1 WITH AN EIGHT-CABLE SUSPENSION SYSTEM

By John S. Mixson and John J. Catherine
Langley Research Center

SUMMARY

Resonant frequencies, mode shapes, and damping of a 1/5-scale dynamic model of the Saturn SA-1 vehicle are presented for two values of stiffness of the eight-cable suspension system and for weight conditions simulating flight times of the full-scale vehicle from lift-off to booster burnout. The eight-cable suspension system used in this investigation was designed to simulate the suspension used in the ground vibration survey of a full-scale Saturn vehicle so that model and full-scale vibration results could be compared on a "same suspension" basis.

It is shown herein that the damping of the model is about the same with the eight-cable suspension as with the two-cable suspension previously used, and that the first bending mode frequency and rocking mode frequency are higher with the eight-cable suspension. The frequencies of the higher modes were not appreciably affected by suspension-system changes. The first bending mode frequency and tip amplitude exhibited nonlinearities similar to those obtained with the two-cable suspension. An increase of shaker force from 13 pounds to 38 pounds decreased the first bending mode frequency by about 4 percent, which is about the same magnitude as the increase of first bending mode frequency caused by stiffening the suspension system.

INTRODUCTION

An investigation of the vibration characteristics of a 1/5-scale dynamic replica of the Saturn SA-1 vehicle has been undertaken at Langley Research Center. The purpose of this investigation is to establish the feasibility of using dynamically scaled models to obtain vibration data which are necessary for the design of complex launch vehicle structures and control systems. In the initial phase of this investigation, the resonant vibration frequencies and the associated mode shapes and damping of the 1/5-scale model of Saturn with the model supported by a two-cable suspension system. The results of this initial phase of the investigation are presented in reference 1 and are shown in reference 2 to be in reasonable agreement with mode shapes and frequencies of the full-scale Saturn, in spite of differences between the two-cable suspension used in the tests of the 1/5-scale model and the eight-cable suspension used in the tests of the full-scale vehicle. The vibration characteristics of the full-scale Saturn vibration test vehicle are described in reference 3.

In the phase of the Saturn model investigation described in this report, the effects of suspension-system variations on the vibration characteristics of the Saturn model have been studied. The resonant frequencies, mode shapes, and damping of the 1/5-scale Saturn model have been determined with the model supported by an eight-cable suspension system. Data were obtained for two values of the suspension-system stiffness and for a range of weight conditions simulating flight time of the full-scale vehicle from lift-off to booster burnout. The eight-cable suspension used in this phase of the Saturn model investigation was designed to simulate the suspension used in the ground vibration survey of a full-scale Saturn vehicle so that model and full-scale vibration results could be compared on a "same suspension" basis.

In this report the 1/5-scale Saturn model, the eight-cable suspension system, and the procedure for determination of the mode shapes, frequencies, and damping of the model are described; and comparisons of these results with results from the model tests with the two-cable suspension system are presented. The vibration characteristics of the model presented herein are compared in reference 4 with results of the full-scale vibration tests.

DESCRIPTION OF THE 1/5-SCALE SATURN MODEL

The 1/5-scale model of Saturn SA-1 is shown suspended in the vibration test tower in figure 1, and a sketch of the model showing its dimensions and the nomenclature used herein is shown in figure 2. A detailed description of the model is given in reference 1.

The Saturn model is 388.6 inches (32 ft., 4.6 in.) in overall length, and weighs about 7,400 pounds when ballasted to simulate the lift-off weight condition. It consists of three stages and a conical payload section; the booster diameter is 52 inches. Water was used in the model to simulate the mass of the fuel and lox; and to account for the density difference between water and fuel or lox, the model water level was adjusted to obtain a properly scaled total weight.

The principal load-carrying structure of the booster (first) stage of the model consists of a 21-inch-diameter center tank which is firmly attached at the lower end to the barrel and outrigger structure, and at the upper end to the spider beam and second-stage adapter structure. Eight 14-inch-diameter outer tanks are arranged around the center tank and are attached to the outriggers and spider beam by two joints at each end of each tank. The full-scale Saturn is designed to carry liquid oxygen in the center tank and in four alternating outer tanks having upper joints which can be adjusted to transmit longitudinal loads, and thus share the load with the center tank. The other four outer tanks of the full-scale Saturn carry fuel and have an upper joint which will not transmit longitudinal load. In this report, the model outer tanks having the type of upper joint which will transmit longitudinal loads will be referred to as "lox" tanks, and the outer tanks having the type of upper joint which will not transmit longitudinal loads will be referred to as "fuel" tanks.

The second stage consists of a cylindrical outer shell which is connected by means of eight radial truss assemblies to an inner water ballast tank. The second stage is attached at the lower end to the second-stage adapter structure only at the junctures of the eight radial trusses with the outer shell. The outer shell thus forms the principal structural member of the second stage; it supports the weight of the ballast tank, which makes up 70 percent of the second-stage weight when water filled, and the weight of the third stage and payload section. The third stage consists simply of a water ballast tank which also supports the nose-cone weight of 14 pounds, which includes the weight of a simulated payload.

APPARATUS

Eight-Cable Suspension System

A view of the Saturn model showing the eight-cable suspension system is presented in figure 3, and a sketch showing pertinent suspension-system dimensions is shown in figure 4. The term "eight cable" is used as a convenient name for this suspension, the principal feature of which is the support of the model by cables attached at the ends of the outriggers. For the model tests described herein, cables were attached to each of the eight outriggers. The cables are tilted outward from the model to allow adequate clearance for the support ring attachments. The system was designed with the cables attached at equal intervals around the support ring so that the points where the cables attach to the support ring and the outrigger would lie in vertical planes through the model longitudinal center line. A close-up view showing the attachment of the cables to the outriggers is shown in figure 5. It can be seen that this suspension does not introduce any appreciable restraint between the outriggers in comparison with the restraint imposed by the support yoke of the two-cable suspension (shown in fig. 7 of ref. 1).

A parallel bank of six springs in series with each cable set is used to reduce the restraint imposed on the model by the suspension. Two series of tests are reported herein; one with the springs in the spring banks and the second with each spring replaced by a rigid $\left(1\frac{1}{2}\right.$ inch by 1/4 inch cross section, $\left.2\frac{1}{2} \text{ inches long}\right)$ steel link. Turnbuckles in series with the cables were used to level the model, center it in the vibration tower, and distribute the weight evenly among the eight support points. Total model weight and weight distribution (among support points) was determined from load cells in series with the cables and springs as shown in figure 4. The springbanks, turnbuckle, and load cells are shown from above in figure 6(a) and from below in figure 6(b).

The springs were calibrated individually and their spring constants were found to be 380 pounds per inch, with a spread among springs of ±14 pounds per inch. The springs were assembled in the banks selectively on the basis of spring constant so that all springbanks would have as nearly as possible the same overall spring constant. The cable assemblies, including the outrigger attachment link, a pair of cables, and a heavy link simulating the lower springbank block, were also calibrated. The load-deflection curves were found to be nonlinear. Cable spring constants for various load invervals are given in the following table:

Load interval, lb	Cable constant, lb/inch
300 to 500	5,550
500 to 700	6,060
700 to 900	6,670
900 to 1,100	7,150

The values for all eight cable pairs are within ±3.5 percent of the given value.

In designing this suspension system to simulate the suspension used to support the full-scale Saturn vibration test vehicle, two factors were considered. First, it was considered important to support the model at the ends of the outriggers as the full-scale vehicle was supported; therefore, the load paths would be the same for model and full-scale vehicles. Second, it was considered important to maintain on the model the same ratio of the first bending mode frequency to the rigid body rocking mode frequency as existed in the full-scale vibration tests. It was found that this ratio was best duplicated by replacing the springs in the springbank by rigid steel links.

Shaker System

An electromagnetic shaker having a capacity of 50 vector pounds of force was used to vibrate the model. It was oriented to apply the force in a plane containing two opposite booster fuel tanks. In all the tests reported herein, the shaker force was applied through a block attached to the bottom of the corrugated barrel as shown in figure 7. With this arrangement, the shaker force was applied at station 20, the gimbal plane. Shaker force was recorded from the output of the load cell shown in figure 7. The frequency of the excitation force was determined from a counter operating on the shaker armature current.

Instrumentation

Vibration deflections, frequency, and damping of the model were determined from unbonded strain-gage accelerometers having natural frequencies ranging from 90 cycles per second to 300 cycles per second and damping of about two-thirds of the critical damping. The location of the accelerometers fixed to the model are shown in figure 8 and typical accelerometer installations on the model are shown in figures 5, 6, and 7. In addition to these fixed accelerometers, an accelerometer provided with a vacuum attachment, such as described in reference 5, was used as a portable pickup to determine the direction of motion of the outer booster tanks. The accelerometer outputs, in addition to the shaker load cell output, was recorded on an oscillograph.

In addition to the instrumentation required to measure dynamic response, strain gages were placed on all four booster outer lox tanks to measure static longitudinal load. Four strain gages were placed around the periphery of the midstation of each tank and were used to measure the compressive load resulting from adjustment of the lox tank upper joints.

PROCEDURE

For each suspension configuration (spring or link), the turnbuckles were adjusted until the model was vertical (checked by transit), centered in the tower structure, and the weight divided as evenly as possible among all eight suspension points. The lox tank upper joints were adjusted until the outer lox tanks supported 40 percent of the upper-stage weight. The remaining 60 percent was supported by the booster center lox tank. In order to raise the frequencies of the shell vibration modes and thus decrease their interference with the bending modes, a pressure of 5 pounds per square inch was maintained in the third-stage and booster outer tanks, and 10 pounds per square inch in the booster center lox tank.

For all tests reported herein, the second and third stages of the model were maintained fully ballasted with water, and different vehicle configurations were obtained by varying the water level in the booster. Results were obtained for five water levels with the spring suspension and three water levels with the link suspension. The measured model weight is given in the following table. These values do not include the weight of the outrigger attachment links (2.0 pounds each), the cables (5.0 pounds for each pair), or the spring banks (23.3 pounds each).

Booster water level, percent full	Simulated flight condition	Measured model weight, lb for -	
		Spring suspension	Link suspension
0	Burnout	2,395	2,425
25	---------------	3,680	-----
48	Maximum dynamic pressure	4,730	4,790
75	---------------	6,090	-----
100	Lift-off	7,330	7,350

The water level at the lift-off weight condition is termed the 100-percent-full condition; the booster tanks are not completely full in this condition. The designations of the other weight conditions are given in terms of percent of the lift-off weight.

At each weight condition for both suspensions, the rigid-body suspension system frequencies and mode shapes were determined, and the results are shown in table I. The mode shapes given in table I are presented in terms of the deflection at station 60 divided by the deflection at station 386 because the suspension-system mode shapes were straight lines within the accuracy of the instruments.

The approximate frequencies of the model resonances were determined by varying the frequency of the shaker input force from about 10 cycles per second to about 50 cycles per second while recording the outputs of the fixed accelerometers on an oscillograph. Each resonance thus discovered was then carefully tuned in and the frequency, mode shape, and damping recorded. The frequency and mode shapes were determined from the fixed accelerometers and the outer tank motions were determined by means of the portable accelerometer. The damping of the model was obtained by cutting the input signal to the shaker at the resonant frequency of interest and recording the output of selected fixed accelerometers on the oscillograph. The amplitudes were read from the oscillograph and plotted on semi-logarithmic paper and a straight line faired through the points. The damping factor g was obtained from the relation:

$$g = \frac{1}{n\pi} \log_e \frac{x_o}{x_n}$$

where

n number of cycles

x_o initial vibration amplitude

x_n amplitude after n cycles

RESULTS AND DISCUSSION

Frequencies, Mode Shapes, and Damping

The experimentally determined resonant frequencies and the associated damping of the 1/5-scale Saturn model with the eight-cable suspension system are summarized in table II. The variation of the resonant frequencies with booster water level is presented in figure 9. The mode shapes are presented in figures 10 to 16.

In figure 9 resonant frequencies of the Saturn model are presented from the tests with the eight-cable spring suspension, the eight-cable link suspension, and the two-cable suspension (obtained from ref. 1). As a convenient way to make the variation of frequency with water level easier to see, the curves shown in this figure were faired through the frequencies of modes obtained with the eight-cable spring suspension (the circular symbols) whose shapes have the same characteristics for the various booster water levels. (At the 48-percent-full water level, no second bending mode was identified with the spring suspensions; therefore, the curves were faired through the frequencies obtained with the eight-cable link suspension.) In nearly every case the mode shapes obtained at approximately the same frequency for different suspension systems and for a given booster water level had the same general characteristics. For example, the mode shapes associated with the curve designated in figure 9 as "first bending mode" are shown in figure 10 to have the same general shape for both suspension systems and for all booster water levels. If the convention of reference 1 is followed, this mode is termed a bending mode because the booster outer tank deflections are predominantly in the same direction with about the same amplitude as the deflection of the center tank. The mode is termed "first" bending because of its resemblance to the first bending mode of a uniform beam. Figures 11 and 12 show that each cluster mode has the same general characteristics for both suspensions and for the various booster water levels. The cluster modes are so named, also following the convention of reference 1, because the booster-outer-tank deflections are predominantly in the opposite direction from the deflections of the center tank. The first cluster mode, shown in figure 11, is distinguished from the second cluster mode, shown in figure 12, by the small curvature in the center-line deflection of the first cluster mode compared with the large curvature of the center-line deflection of the second cluster mode. At booster water levels up to 48 percent full, the Saturn model exhibited two separate responses with mode shapes which could be called second bending modes. One group of these modes is designated "second bending mode, group 1," and is shown in figure 13, and the second group is designated "second bending mode, group 2" and is shown in figure 14. Figures 13 and 14 show that the booster-outer-tank deflections in both groups of modes are predominantly in the same direction as the center-tank deflection and, thus, in the convention of reference 1, both groups of modes are bending modes. For this report the modes were separated into the groups on the basis of the mode shape of the second-stage inner tank. The mode shapes placed in group 1 were those which had relatively small curvature in the second-stage inner tank, and those placed in group 2 had larger curvature in the second-stage inner tank. An exception, and also a mode which had a somewhat different shape for the different suspensions, is shown in figure 13(a). The mode shown in figure 13(b) for a link suspension has large curvature in the second-stage inner tank but was included in group 1 because its frequency was nearly identical to that of the corresponding mode with the spring suspension, shown in figure 13(a) for a spring suspension. Figures 13 and 14 both show large differences between the deflection of the second-stage inner tank (the triangular symbols) and the second-stage outer shell (the circular symbols between stations 196 and 280). This effect is attributed to shell motion in the second stage such as described in reference 1. The outstanding characteristic shared by the outer tank modes, shown in figure 15, is the large deflections of the booster outer tanks compared with the deflection of the center line. The miscellaneous mode shapes shown in figure 16 are associated with the resonances which appeared only at one weight condition; the frequencies of these modes are shown in figure 9 without any faired curves.

Comparison of the number of modes identified with the two-cable suspension (the square symbols in fig. 9) with the number identified with the eight-cable spring suspension (the circular symbols) shows that about 10 more modes were identified with the eight-cable suspension. This difference is thought to be due primarily to greater instrument coverage rather than to a difference of suspension. The test procedure with both suspensions consisted of a sweep of shaker frequency over the desired range while the outputs of the fixed accelerometers were recorded. For the two cable tests the model had accelerometers fixed only to the booster center tank and the upper stages; however, for the eight-cable tests there were additional accelerometers fixed to the booster outer tanks. Thus, modes which consisted primarily of outer tank motion, with small center-line motion, would not be as easily discovered in the two-cable tests (with no outer tank accelerometer) as in the eight-cable tests. Examination of the mode shapes associated with the frequencies which were identified in the eight-cable tests but not in the two-cable tests (the outer-tank modes, fig. 15, for example) shows this to be the case; most of these modes exhibit large outer tank deflections and relatively small center-line deflection.

The effect of suspension system changes on the frequency of the first bending mode is shown in figure 9. Comparison of the frequencies obtained for the first bending mode with the two-cable suspension (the square symbols) with those obtained with the eight-cable-spring suspension (the circular symbols) shows a maximum increase of about 4.6 percent. The eight-cable-link suspension is shown to increase the first vehicle bending mode frequency by about 10 percent over the two-cable frequencies. The ratios of the rigid-body rocking frequency to the first bending mode frequency for the two-cable suspension, the eight-cable spring, and the eight-cable link suspensions were 0.02, 0.08, and 0.15, respectively. The fact that this ratio is the smallest for the two-cable suspension indicates that the first vehicle bending mode frequency obtained with two-cable suspension has the smallest suspension effects and is the nearest of these three to the free-free frequency of the model. The fact that the frequencies of the higher modes shown in figure 9 do not display any consistent variation with suspension-system changes indicates that the suspension system has little effect on the frequencies of these higher modes.

In table III values of the damping factor g are given for the first four principal modes at five weight conditions with the two-cable suspension and with the eight-cable suspension with springs and with links. Where two values of g are given for a particular mode, weight condition, and suspension, the larger value was measured early in the decrement whereas the smaller value was measured after the vibration amplitude had decreased considerably. Thus, table III shows that the model damping decreased as the vibration amplitude decreased. Two values of damping are shown in table III for several modes with both suspension systems which indicate that the variation of damping with vibration amplitude is not primarily a suspension-system effect. Table III also shows that for most modes the damping values obtained with the two different suspensions are of the same order of magnitude.

Nonlinear Effects

A short investigation of the effect of shaker-force magnitude on the model response in the frequency range of the first bending mode has been conducted and some of the results are shown in figure 17. The variation with frequency of the ratio of tip deflection to shaker force is shown for shaker input forces of 13 and 38 pounds for the eight-cable suspension with springs (fig. 17(a)) and for the eight-cable suspension with links (fig. 17(b)). Figure 17(a) shows that the effect of the force increase from 13 to 38 pounds is to decrease the magnitude of the peak and to shift the frequency of the peak from 10.65 cycles per second to 10.2 cycles per second. A decrease of frequency with increase of force was also reported in reference 1 with the two-cable suspension system. The decrease of frequency shown in figure 17(a) is about 4 percent, which is about the same magnitude as the difference shown in figure 9 between the first mode frequencies obtained with the two-cable and eight-cable spring suspensions. (The first-mode frequencies shown in figure 9 were obtained with shaker force inputs of less than 18 pounds except for the first mode with the two-cable suspension system at the booster empty and full conditions.) A more complicated effect of shaker force variation is shown in figure 17(b). For each force there are three distinct amplitude peaks, and the increase of force not only shifts the frequency of each peak downward but also changes the magnitude of each peak differently. Thus, with the highest peak taken as the first mode, the increase of force from 13 pounds to 38 pounds decreased the frequency from 11.6 to 10.8 cycles per second, a change of about 7 percent. It can be concluded from figure 17 that changes of the input force can cause variations of the first bending mode frequency which are about the same magnitude as changes caused by suspension system changes.

Frequency-response curves were also obtained with the booster 75 percent full, and their overall appearance was similar to the appearance of the curves shown in figure 17(a). The maximum deflection in inches per pound and the corresponding frequency obtained from these curves, as well as the curves of figure 17, are shown in the following table:

Weight, percent full	Force, lb	Frequency of peak, cps	Maximum deflection, in./lb
	Eight-cable link suspension		
75	13	12.8	0.0044
75	38	12.33	.0044
100	13	11.10	.0024
100	13	11.6	.0030
100	38	10.8	.0026
100	38	11.6	.0018
	Eight-cable spring suspension		
75	13	12.35	0.0036
75	38	11.80	.0033
100	13	10.65	.0060
100	38	10.2	.0040

This table shows that for both suspension systems and both weight conditions the effect of increasing the shaker force is to decrease the frequency at the maximum deflection, and to either not change or decrease the maximum deflection in inches per pound. These nonlinear effects are similar in character to those obtained from the model with the two-cable suspension (described in ref. 1); therefore, the nonlinearities are not entirely caused by a particular suspension system or by some characteristic of a particular weight condition.

CONCLUDING REMARKS

An investigation of the vibration characteristics of a 1/5-scale model of the Saturn SA-1 vehicle supported by an eight-cable suspension system has been performed at Langley Research Center and the results are reported herein. The suspension system used in this investigation was designed to simulate the suspension used in the vibration survey of a full-scale Saturn at Marshall Space Flight Center.

Comparisons are presented herein of the frequencies and damping of the model with an eight-cable suspension with those obtained with a two-cable suspension. These comparisons show that the model had approximately the same damping with both suspensions and the first bending mode frequency increased as the rigid-body rocking frequency was increased. The first bending mode frequency was lowest with the two-cable suspension, was about 4.6 percent higher with the eight-cable spring suspension, and was about 10 percent higher with the eight-cable link suspension; the respective values of the ratio of the rigid body rocking frequency to the first bending mode frequency were 0.02, 0.08, and 0.15. The first bending mode frequency obtained with the two-cable suspension has the smallest suspension effects (because the rocking-bending frequency ratio is smallest) and is therefore the nearest of these three to the free-free frequency of the model. The higher mode frequencies appeared to be unaffected by the suspension-system changes.

The resonant frequency and tip amplitude of the first bending mode of the model with the eight-cable suspension are shown to exhibit nonlinear characteristics similar to those obtained from the model with the two-cable suspension. An increase of shaker force from 13 pounds to 38 pounds decreased the first bending mode frequency by about 4 percent, which is about the same magnitude as the increase of first-mode frequency caused by stiffening the suspension system.

Langley Research Center,
National Aeronautics and Space Administration,
Langley Station, Hampton, Va., June 5, 1964.

REFERENCES

1. Mixson, John S., Catherine, John J., and Arman, Ali: Investigation of the Lateral Vibration Characteristics of a 1/5-Scale Model of Saturn SA-1. NASA TN D-1593, 1963.

2. Runyan, Harry L., and Leonard, Robert W.: Research, Design Considerations, and Technological Problems of Structures for Launch Vehicles. Proceedings of the NASA-University Conference on the Science and Technology of Space Exploration, vol. 2, NASA SP-11, 1962, pp. 487-532. (Also available as NASA SP-28.)

3. Propulsion and Vehicle Engineering Division: Experimental Vibration Program on a Full Scale Saturn Space Vehicle. Appendix B of Saturn Quarterly Progress Report. MPR-SAT-62-3, NASA George C. Marshall Space Flight Center, Jan.-Mar. 1962.

4. Mixson, John S., and Catherine, John J.: Comparison of Experimental Vibration Characteristics Obtained From a 1/5-Scale Model and From a Full-Scale Saturn SA-1. NASA TN D-2215, 1964.

5. Brooks, George W.: Techniques for Simulation and Analysis of Shock and Vibration Environment of Space Flight Systems. Experimental Techniques in Shock and Vibration, Will J. Worley, ed., ASME, c.1962, pp. 93-105.

TABLE I.- RIGID BODY MODES OF THE 1/5-SCALE SATURN MODEL

WITH THE EIGHT-CABLE SUSPENSION

Weight	Suspension	Pendulum mode		Rocking mode	
		Frequency, cps	$\bar{x}_{60}$ (*)	Frequency, cps	$\bar{x}_{60}$ (*)
Empty	Spring Link	0.24 .23	0.39 .75	1.60 2.50	-0.92 -1.00
25 percent full	Spring	0.23	0.59	1.00	-0.62
48 percent full	Spring Link	0.24 .25	---- 0.68	0.95 1.85	-0.44 -.43
75 percent full	Spring	0.24	----	0.93	-0.40
100 percent full	Spring Link	0.23 .24	---- ----	0.93 1.76	-0.36 -.30

*$\bar{x}_{60}$: Deflection at station 60 divided by deflection at station 386.

TABLE II.- SUMMARY OF FREQUENCIES AND DAMPING OF THE 1/5-SCALE SATURN MODEL WITH THE EIGHT-CABLE SUSPENSION SYSTEM

Mode	Booster, empty				Booster, 25 percent full		Booster, 48, percent full				Booster, 75 percent full		Booster, 100 percent full			
	Frequency, cps		Damping, g		Frequency, cps	Damping, g	Frequency, cps		Damping, g		Frequency, cps	Damping, g	Frequency, cps		Damping, g	
	Spring	Link	Spring	Link	Spring suspension		Spring	Link	Spring	Link	Spring suspension		Spring	Link	Spring	Link
Fuel tank no. 1	----	----	------------	-----	25.2	0.006	----	----	-------------	-------------	----	-------------	9.1	9.1	-----	0.01
First bending	14.0	14.7	*0.032, 0.015	0.03	13.8	*.029, .016	13.6	14.1	*0.030, 0.013	*0.033, 0.012	12.3	*0.037, 0.015	10.7	11.7	0.030	.01
First bending and outer tank	----	----	------------	-----	21.0	------------	14.7	15.5	-------------	-------------	----	-------------	----	----	-----	-----
Booster	----	----	------------	-----	----	------------	20.8	20.8	-------------	-------------	----	-------------	----	----	-----	-----
First cluster	----	----	------------	-----	31.8	------------	25.5	26.3	-------------	*.030, .013	20.8	-------------	18.7	18.9	-----	-----
Second cluster	----	----	------------	-----	47.0	.013	34.7	35.0	-------------	-------------	27.7	.012	23.9	24.6	.015	.018
Second bending	45.1	45.8	*.028, .011	.024	38.5	------------	----	38.5	-------------	-------------	36.2	.017	30.8	30.8	-----	-----
Second bending	50.1	50.0	------------	-----	43.7	------------	----	43.4	-------------	-------------	----	-------------	----	----	-----	-----
Second bending and outer tank	----	----	------------	-----	29.6	.029	----	----	-------------	-------------	----	-------------	----	----	-----	-----
Outer tank second bending	----	----	------------	-----	----	------------	----	----	-------------	-------------	----	-------------	41.1	41.5	-----	-----
Third bending	----	----	------------	-----	----	------------	----	----	-------------	-------------	----	-------------	47.5	----	-----	-----
Third cluster	----	----	------------	-----	50.4	------------	----	----	-------------	-------------	----	-------------	----	----	-----	-----

*The large value of g was measured for large values of decaying amplitude; the small value of g was measured for smaller amplitudes.

TABLE III.- COMPARISON OF DAMPING OF 1/5-SCALE SATURN MODEL

WITH TWO-CABLE AND EIGHT-CABLE SUSPENSIONS

[Values given are for $g = \left(\frac{1}{n\pi}\right)\log_e \frac{x_o}{x_n}$]

	Booster, empty (burnout)	Booster, 25 percent full	Booster, 48 percent full (maximum Q)	Booster, 75 percent full	Booster, 100 percent full (liftoff)
First bending mode					
Two-cable	*0.030, 0.017	0.050	*0.032, 0.017	0.020	*0.033, 0.025
Eight-cable: Spring	*.032, .015	*.029, .016	*.030, .013	*.037, .015	.030
Eight-cable: Link	.030	-----------	*.033, .012	-----------	.01
First cluster mode					
Two-cable	-----------	-----------	*0.023, 0.011	*0.025, 0.015	0.017
Eight-cable: Spring	-----------	-----------	-----------	.021	-----------
Eight-cable: Link	-----------	-----------	*.030, .013	-----------	-----------
Second cluster mode					
Two-cable	-----------	-----------	-----------	*0.022, 0.016	0.014
Eight-cable: Spring	-----------	0.013	-----------	.012	.015
Eight-cable: Link	-----------	-----------	-----------	-----------	.018
Second bending mode					
Two-cable	*0.046, 0.032	-----------	-----------	*0.039, 0.019	-----------
Eight-cable: Spring	*.028, .011	-----------	-----------	.017	-----------
Eight-cable: Link	.024	-----------	-----------	-----------	-----------

*The large value of g was measured for large values of decaying amplitude; the small value of g was measured for smaller amplitudes.

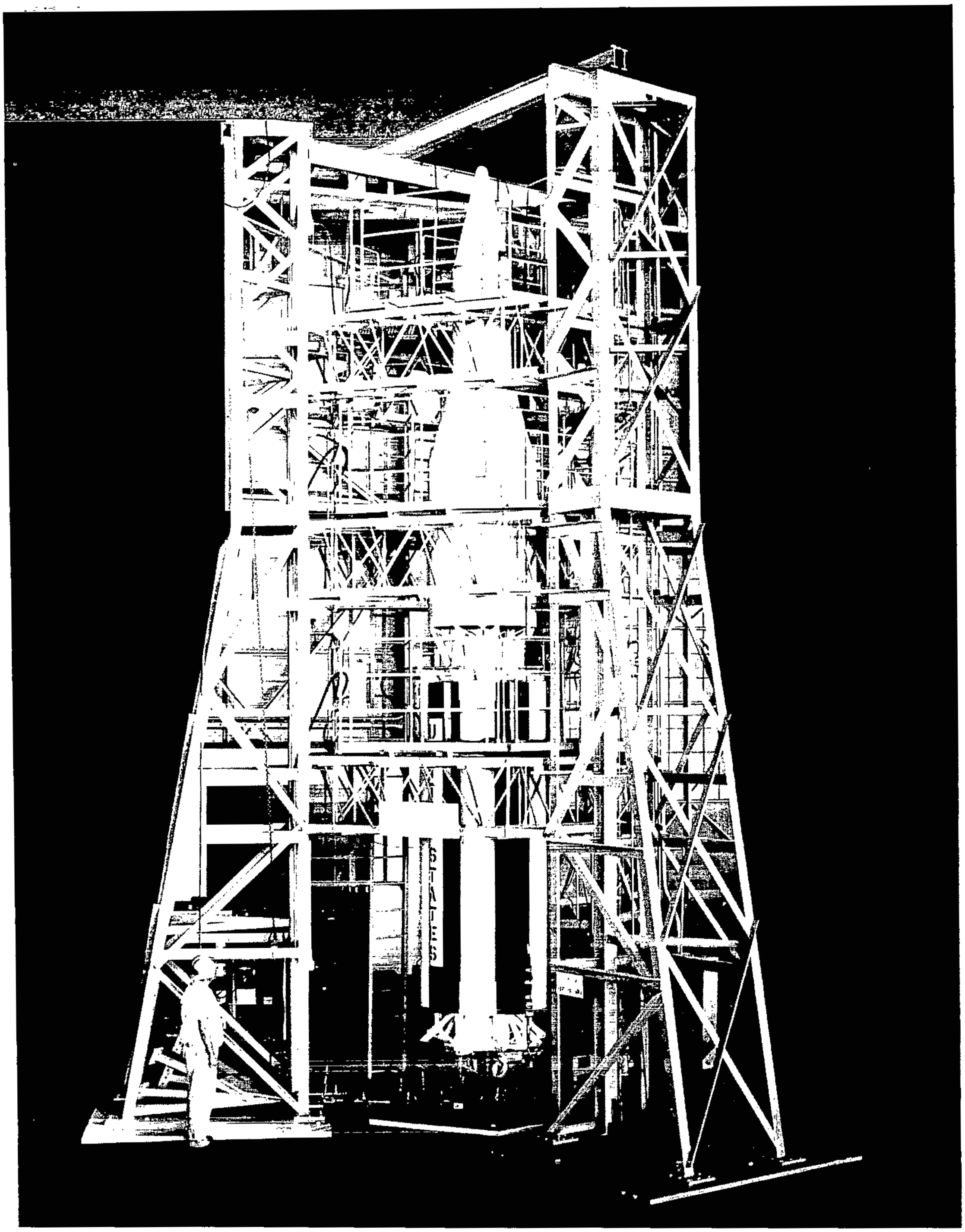

L-61-4079

Figure 1.- The 1/5-scale Saturn model suspended in vibration testing tower.

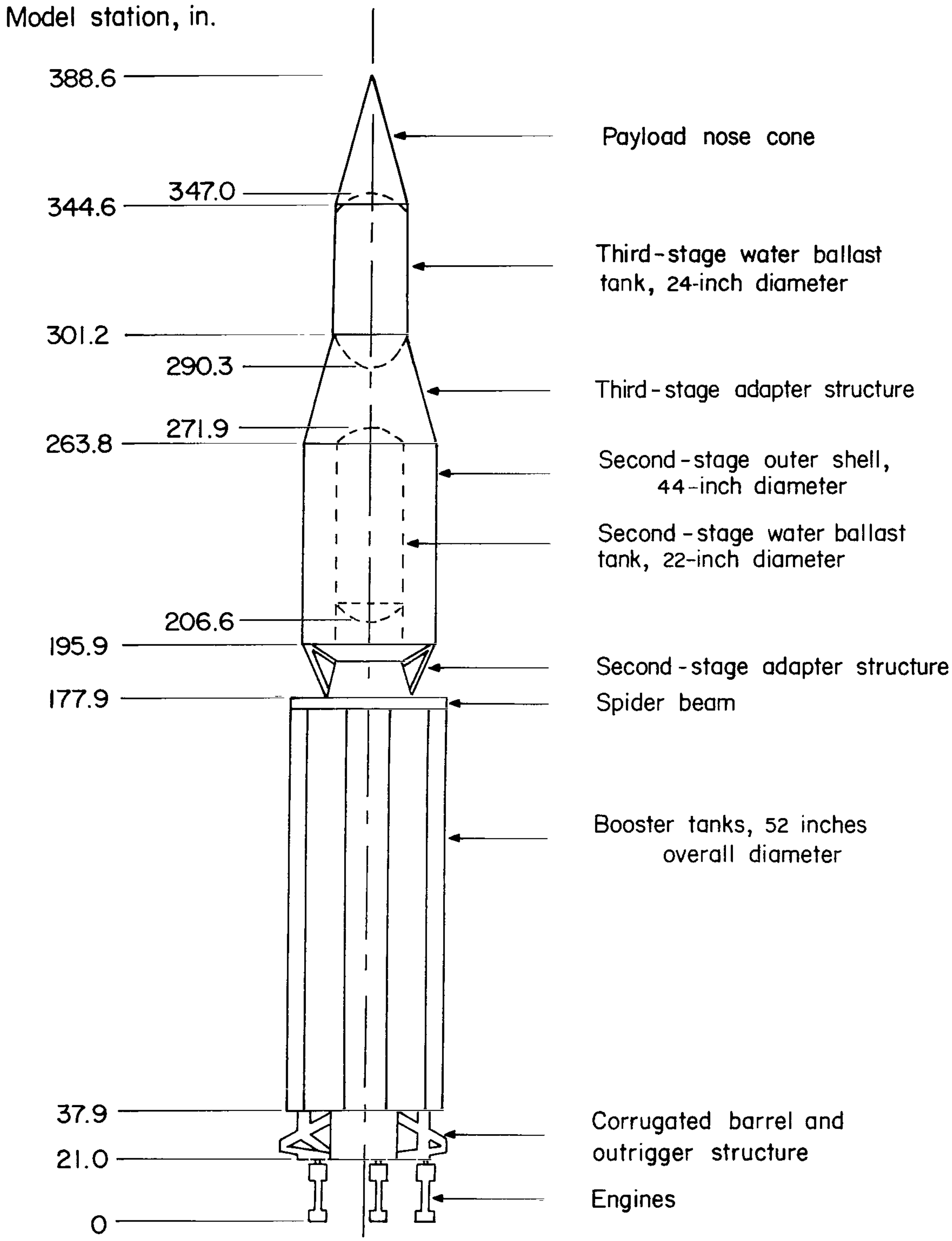

Figure 2.- General configuration dimensions, and nomenclature of 1/5-scale model of Saturn SA-1.

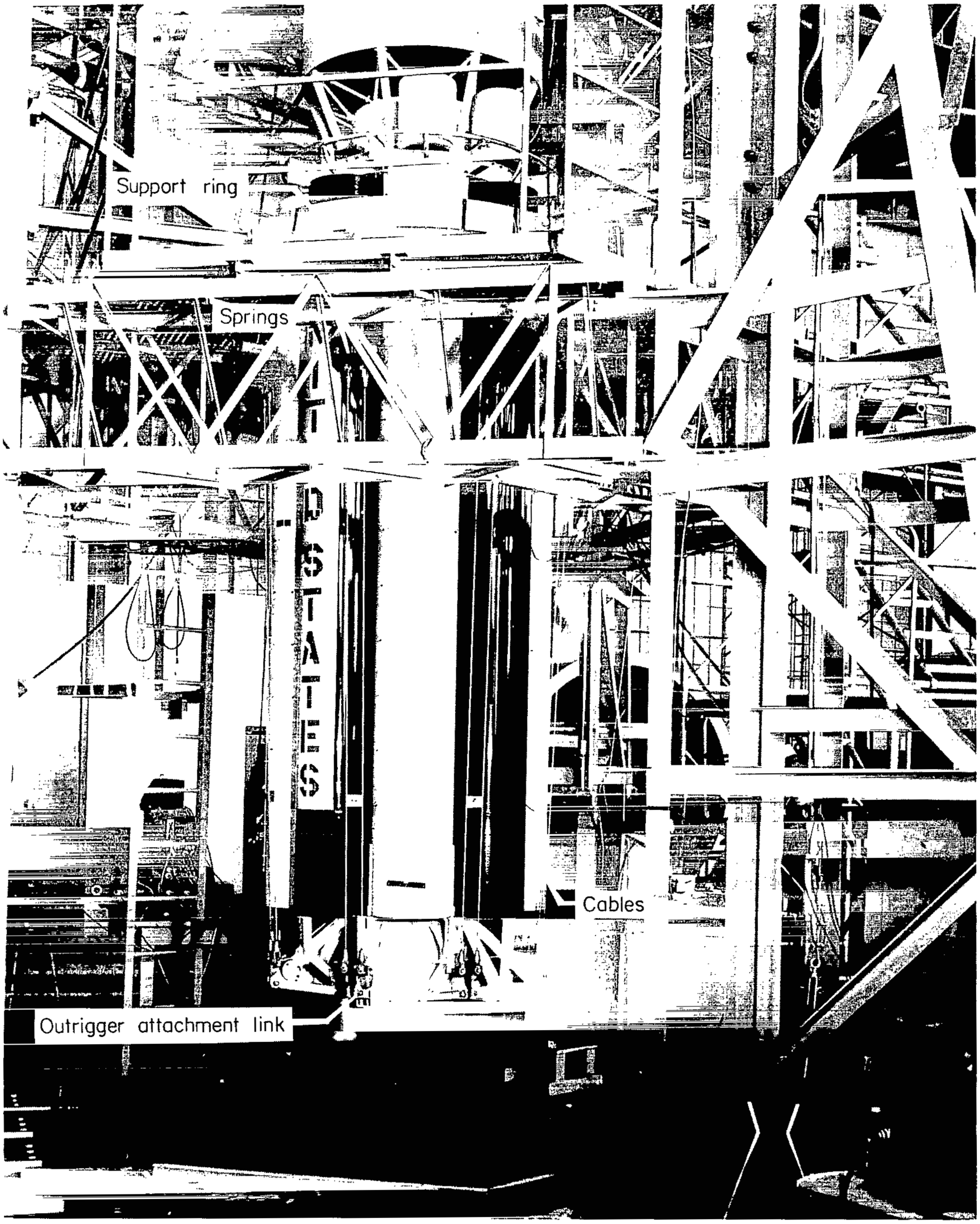

L-62-5089.1
Figure 3.- Booster area of 1/5-scale Saturn model showing eight-cable suspension system.

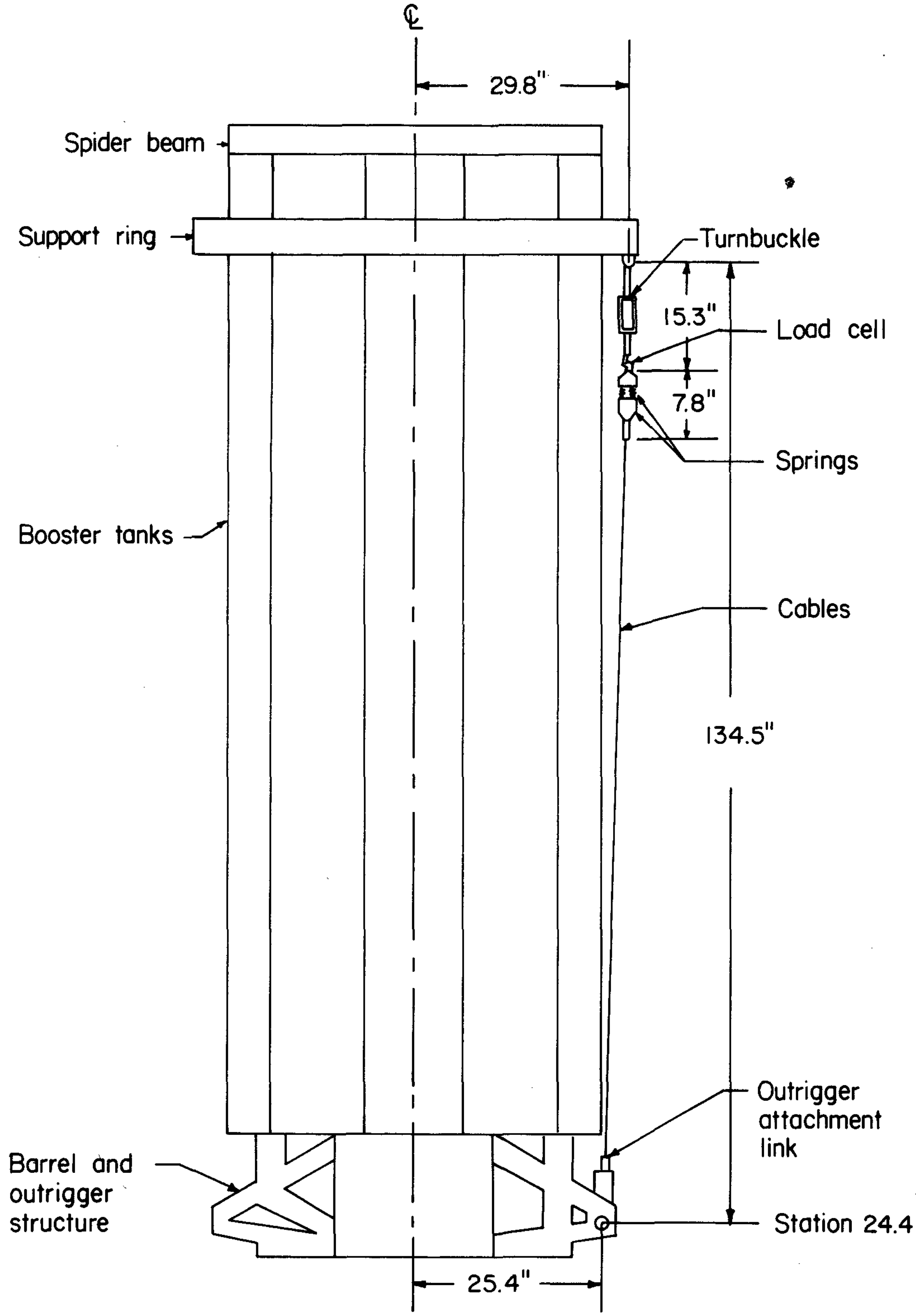

Figure 4.- Eight-cable suspension-system dimensions. All dimensions are in inches.

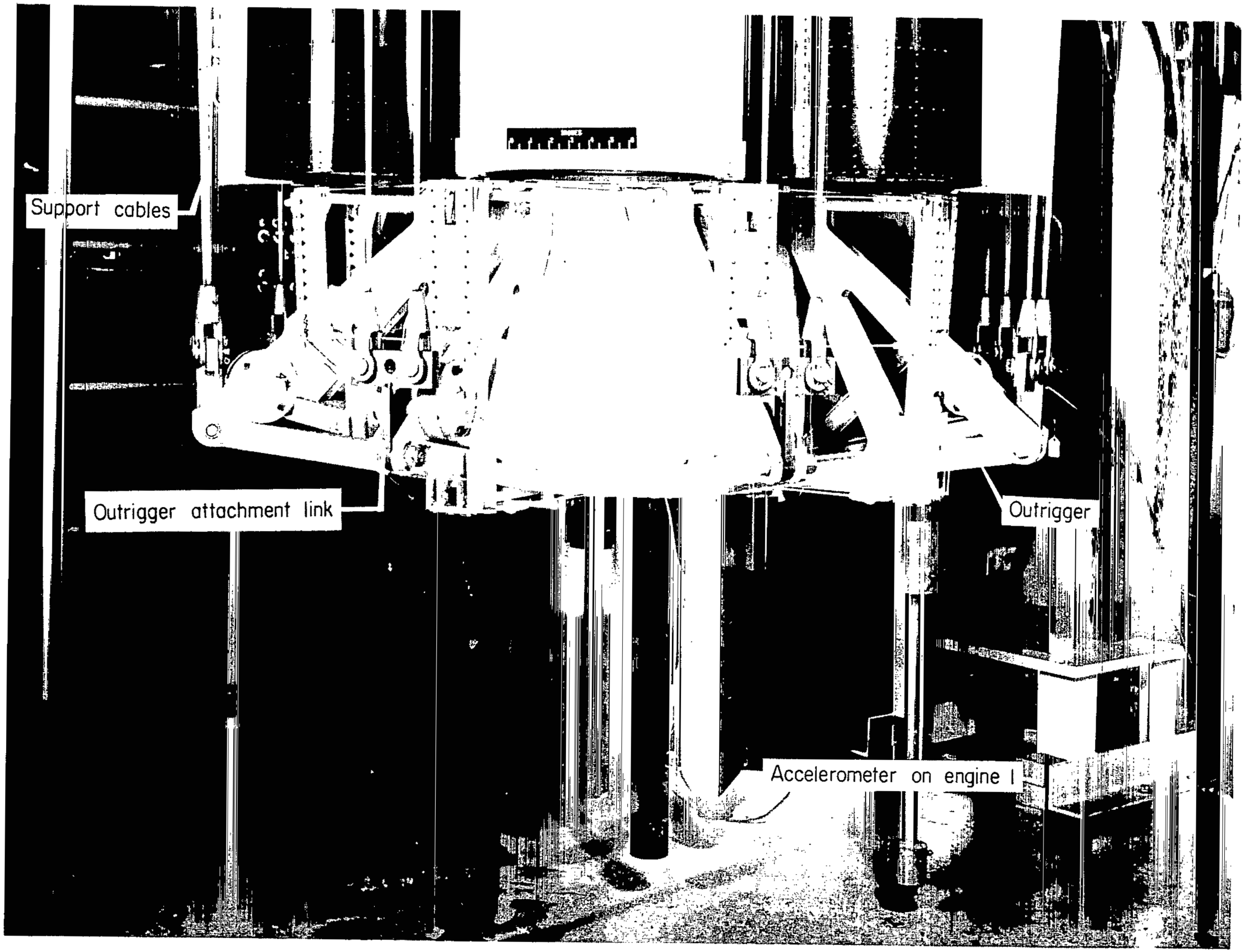

Figure 5.- Eight-cable suspension attachments to outriggers of 1/5-scale Saturn model. L-62-5095.1

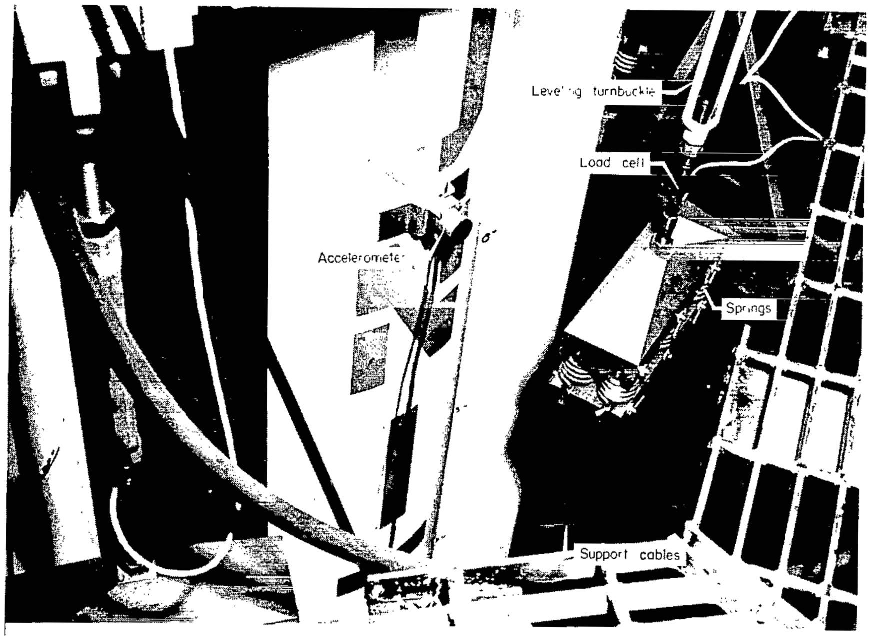

(a) Top view. L-62-5099.1

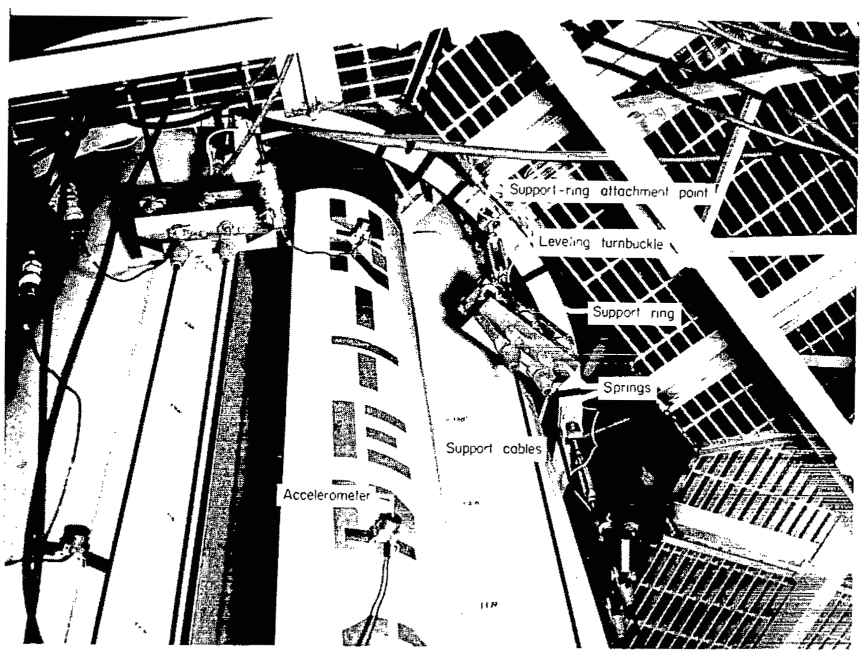

(b) Bottom view. L-62-5098.1

Figure 6.- Spring bank area of eight-cable suspension.

L-62-5100.1

Figure 7.- Barrel area of 1/5-scale Saturn model showing shaker-rod attachment.

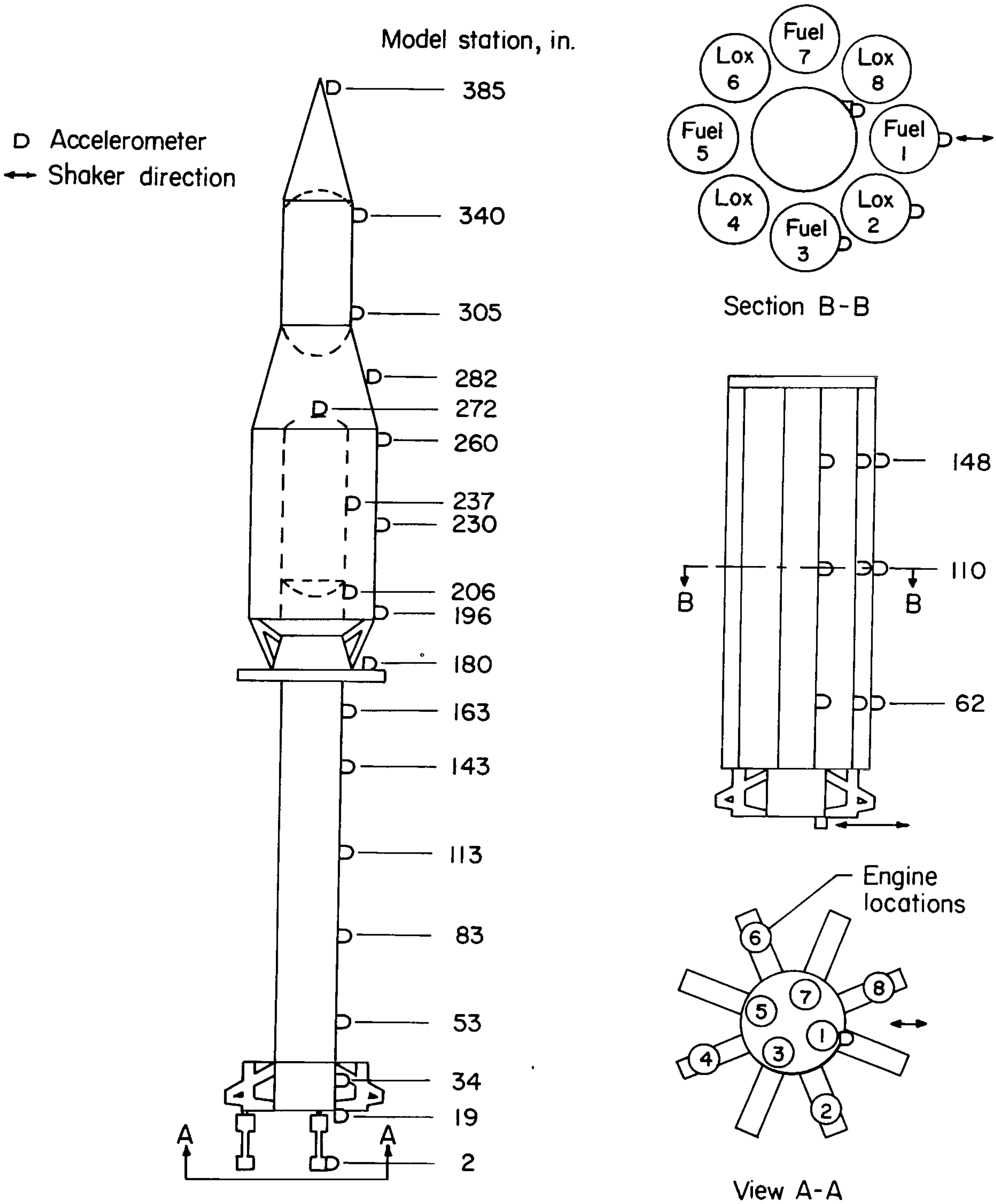

Figure 8.- Location of accelerometers on 1/5-scale Saturn model for tests with the eight-cable suspension.

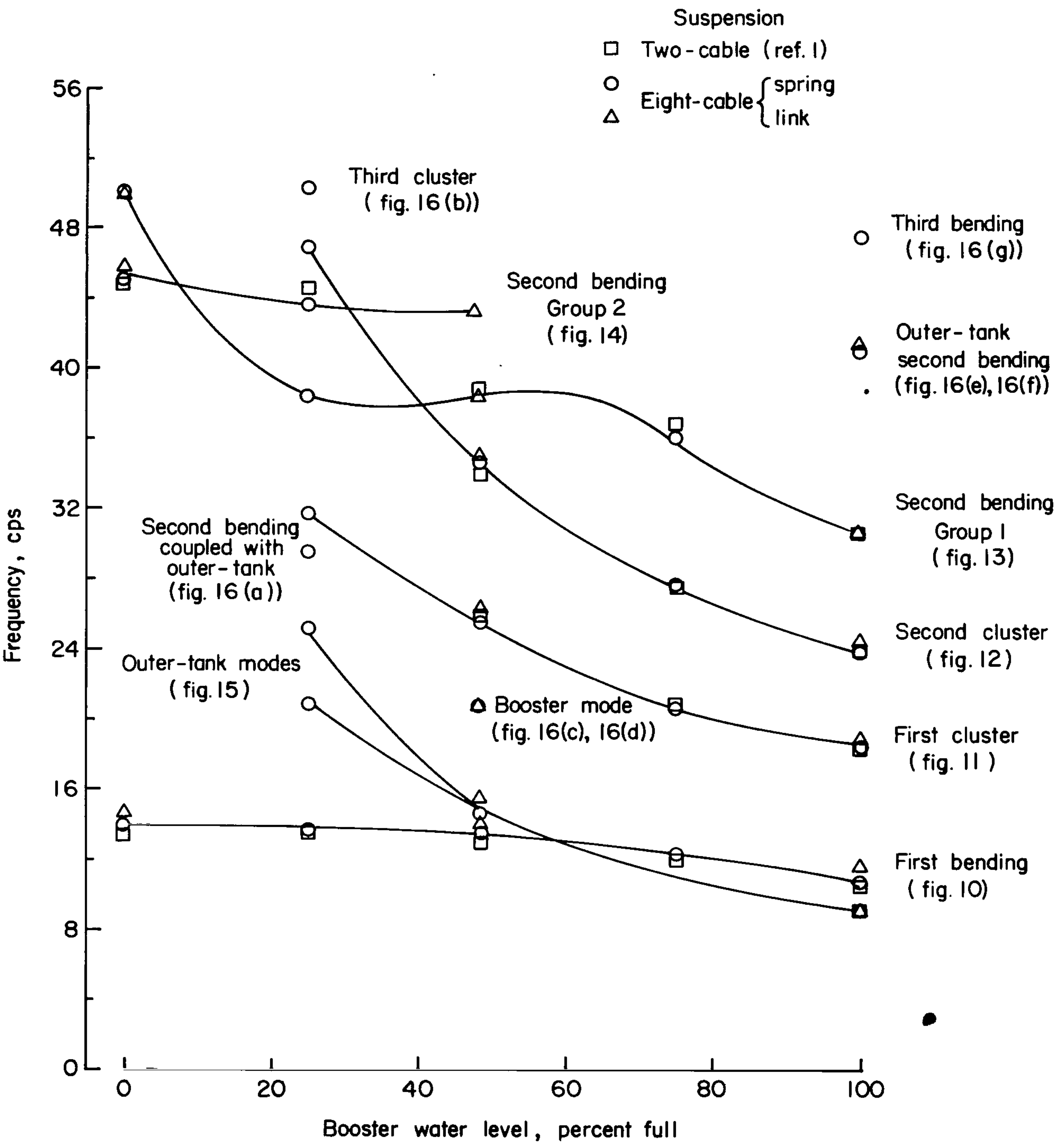

Figure 9.- Variation of resonant frequencies of the 1/5-scale Saturn model with booster water level.

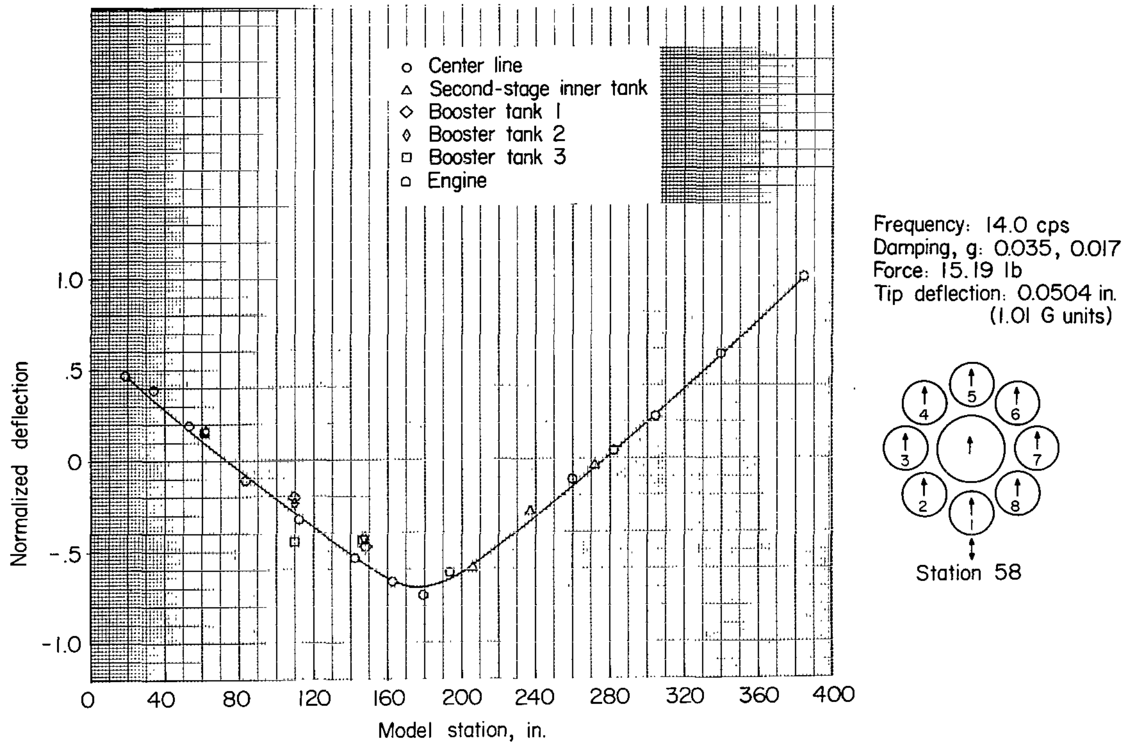

(a) Booster tank empty; spring suspension.

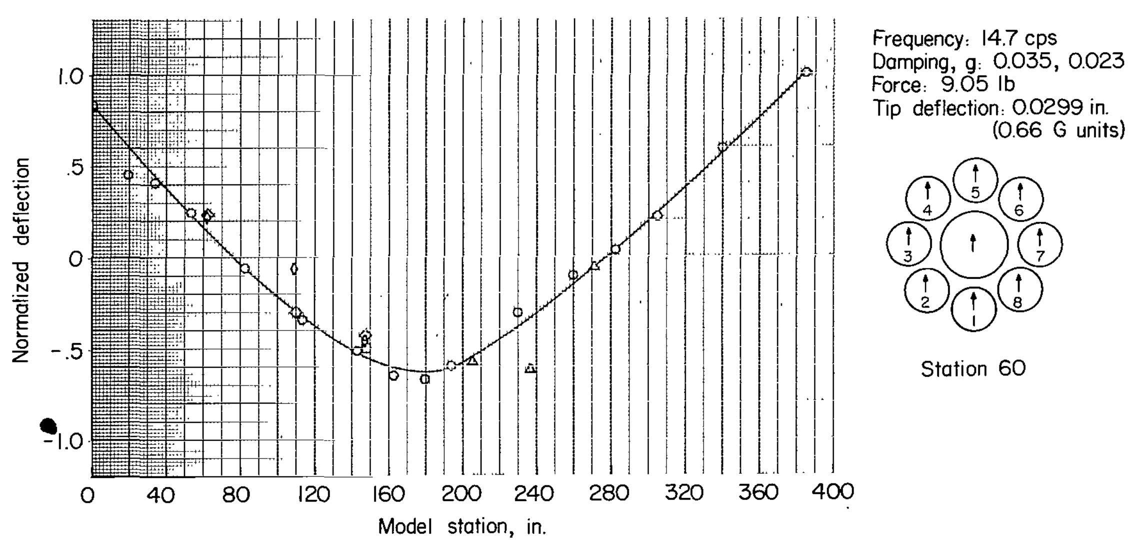

(b) Booster tank empty; link suspension.

Figure 10.- First bending mode of 1/5-scale Saturn model.

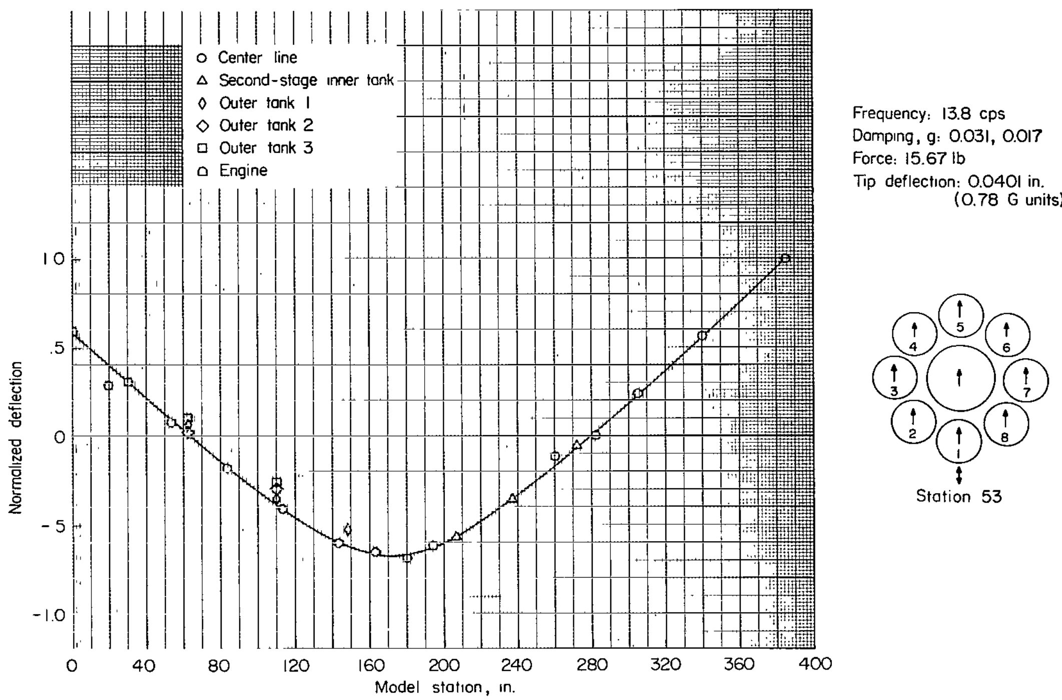

(c) Booster tank 25 percent full; spring suspension.

Figure 10.- Continued.

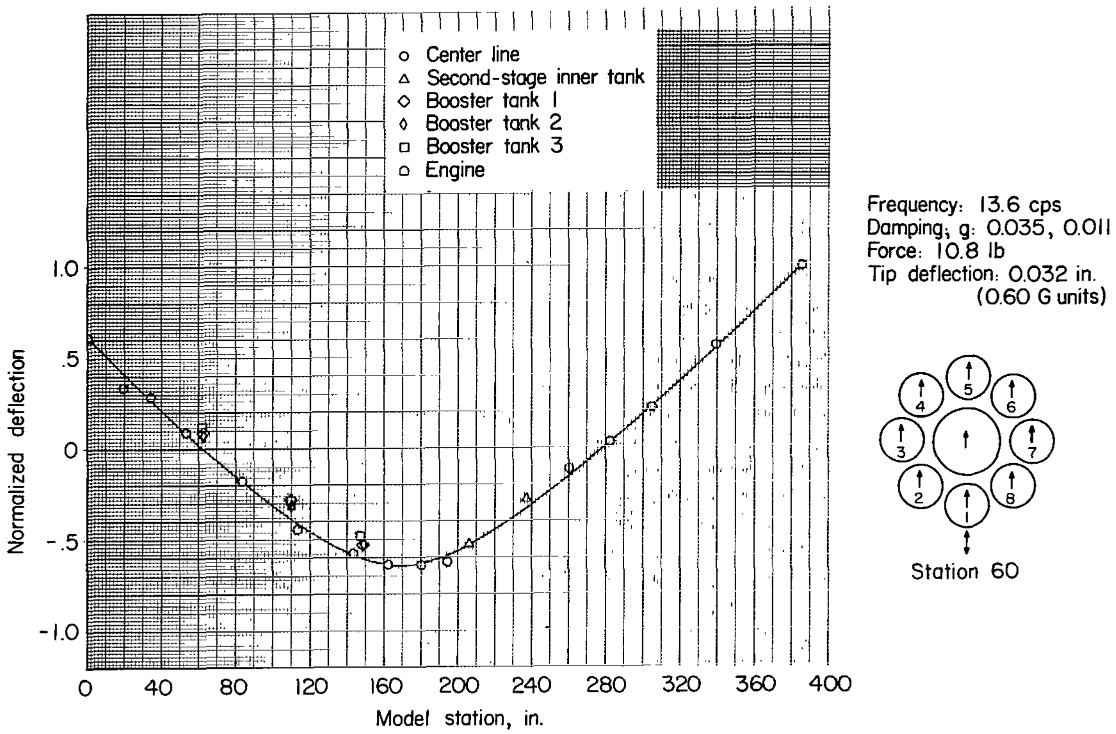

(d) Booster tank 48 percent full; spring suspension.

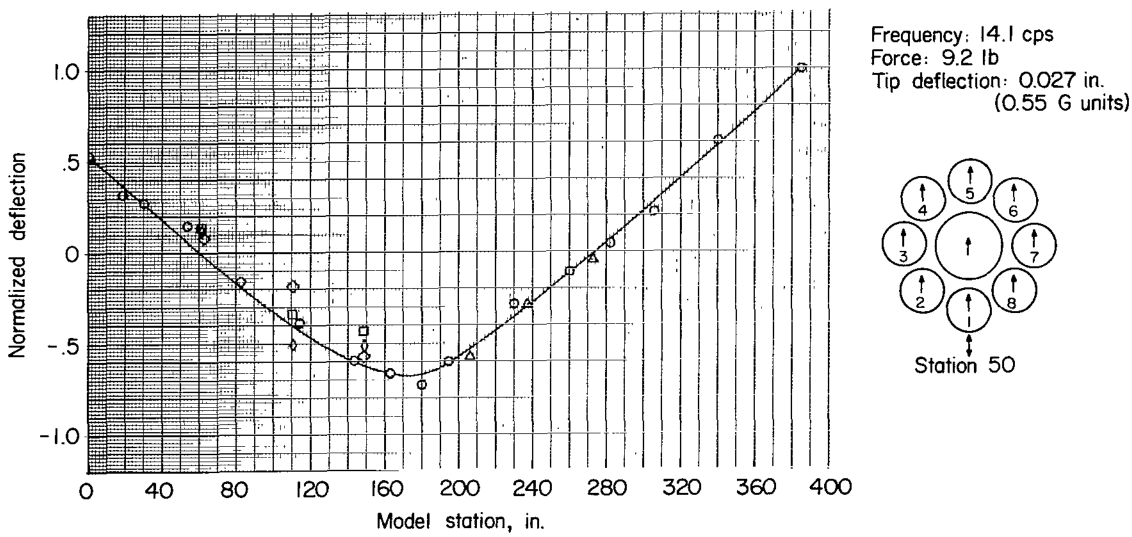

(e) Booster tank 48 percent full; link suspension.

Figure 10.- Continued.

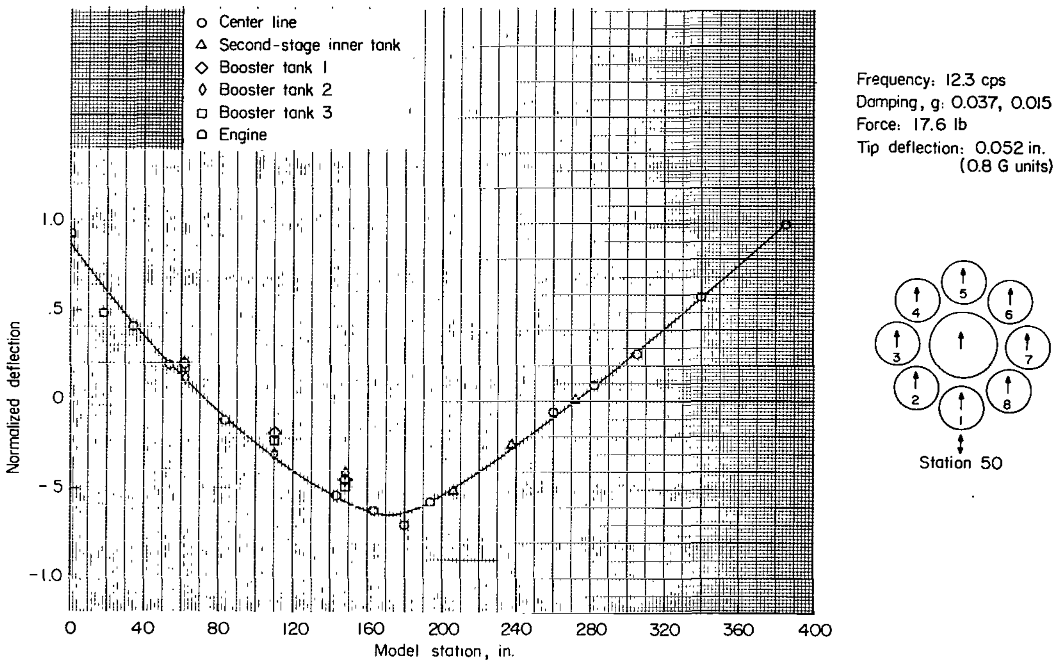

(f) Booster tank 75 percent full; spring suspension.

Figure 10.- Continued.

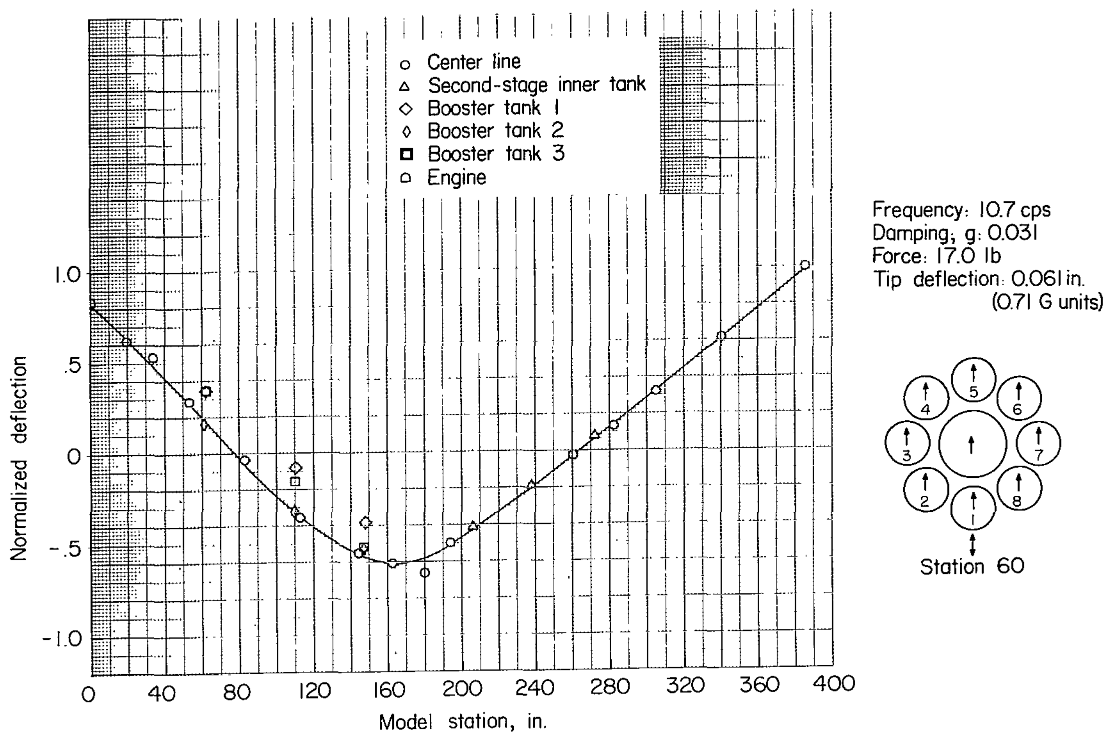

(g) Booster tank full; spring suspension.

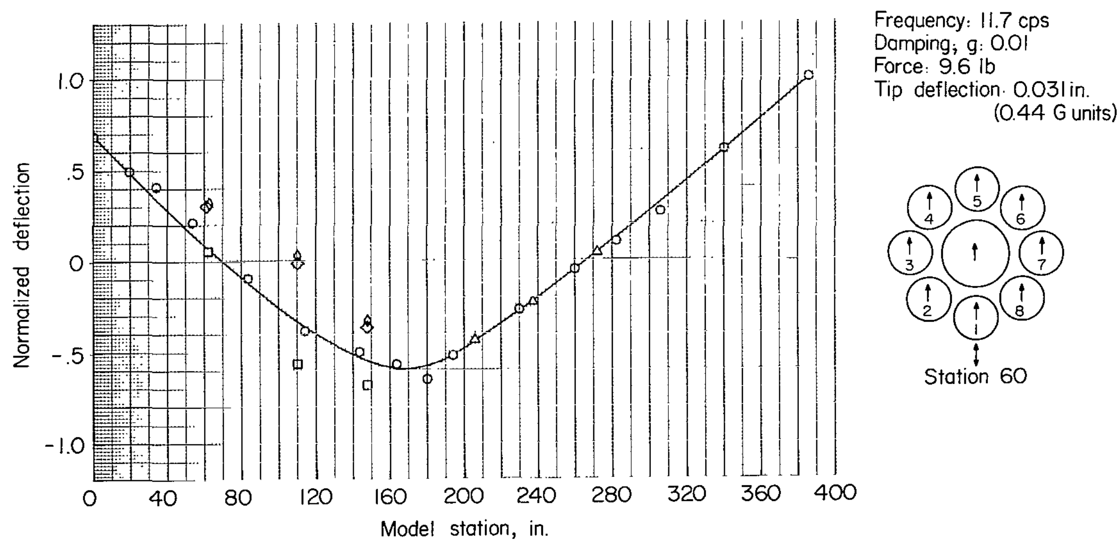

(h) Booster tank full; link suspension.

Figure 10.- Concluded.

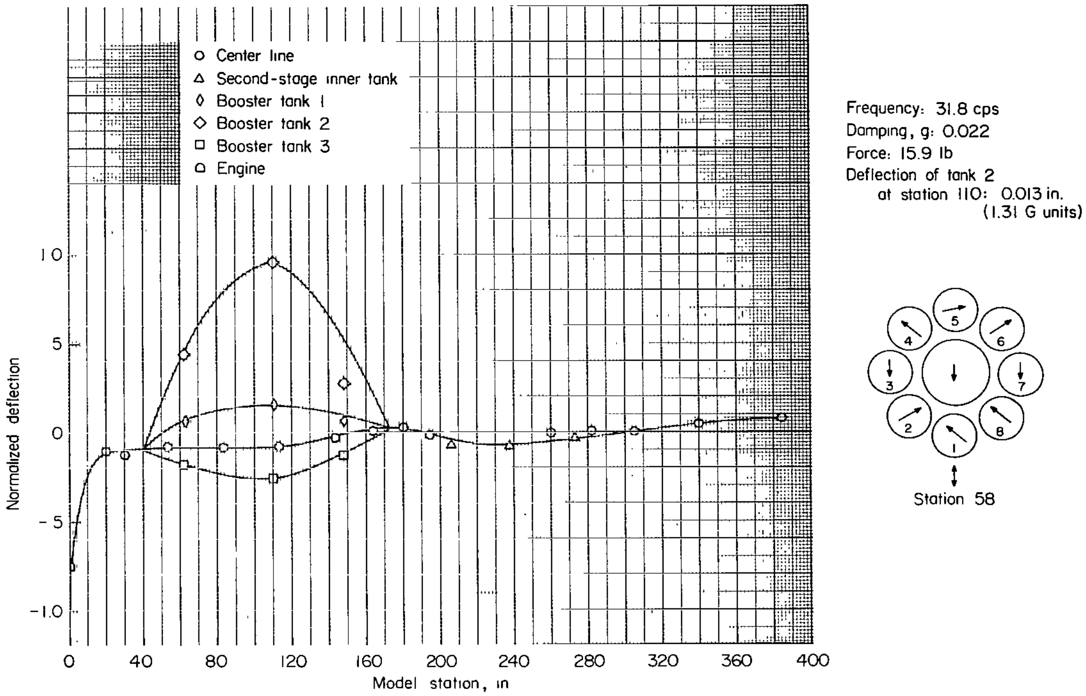

(a) Booster tank 25 percent full; spring suspension.

Figure 11.- First cluster mode of 1/5-scale Saturn model.

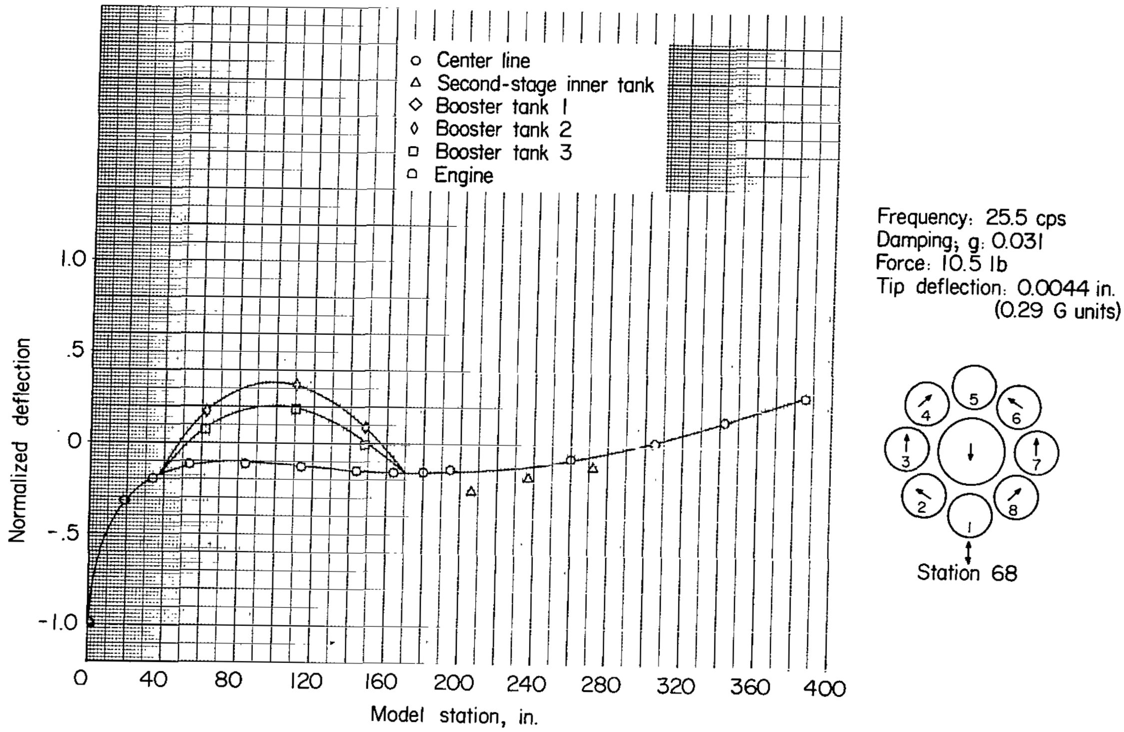

(b) Booster tank 48 percent full; spring suspension.

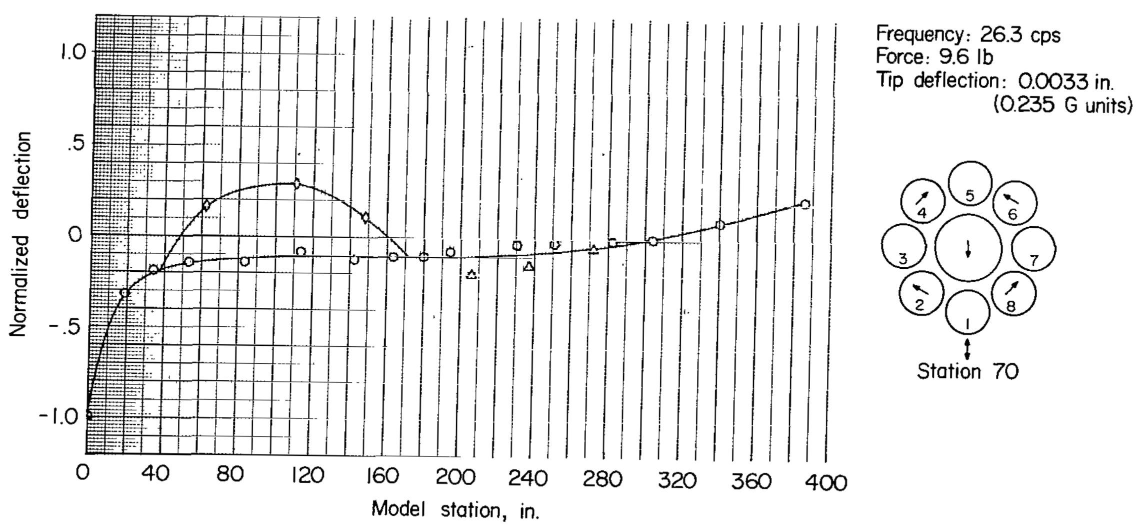

(c) Booster tank 48 percent full; link suspension.

Figure 11.- Continued.

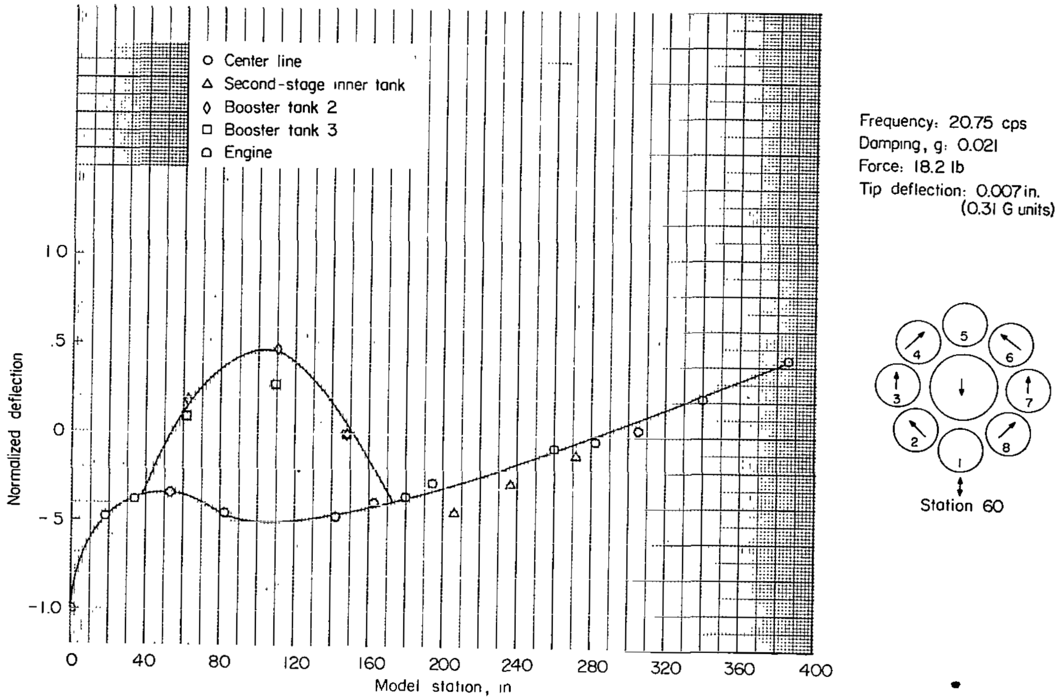

(d) Booster tank 75 percent full; spring suspension.

Figure 11.- Continued.

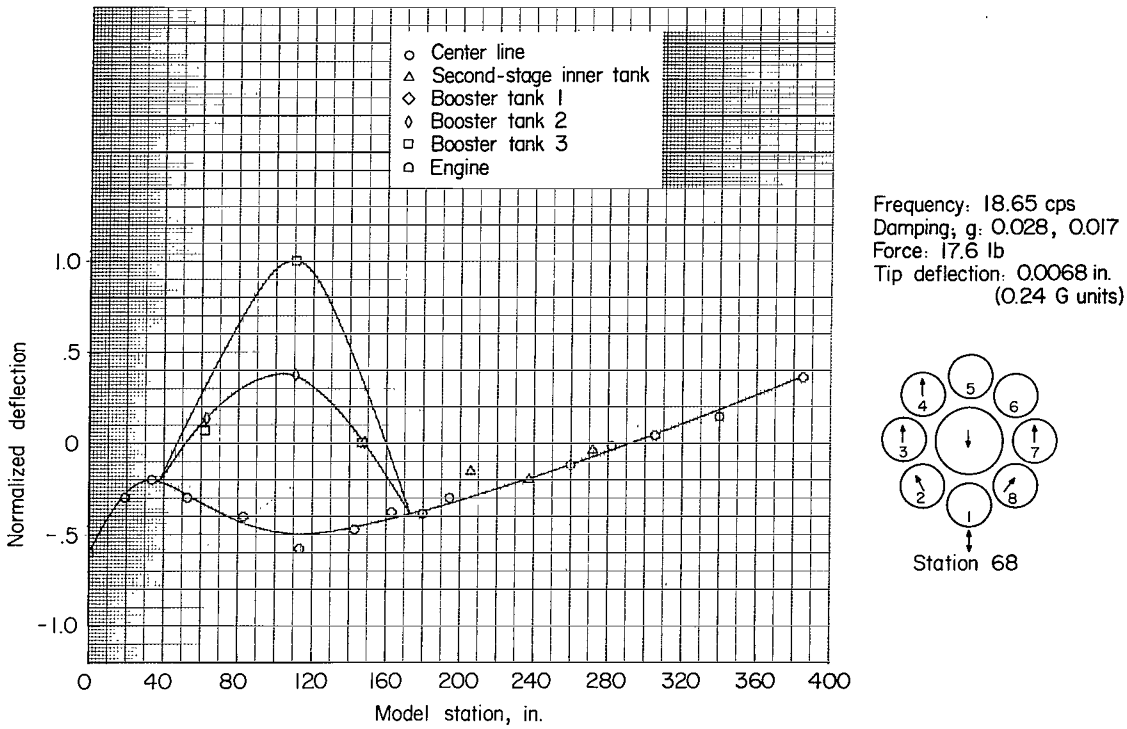

(e) Booster tank 100 percent full; spring suspension.

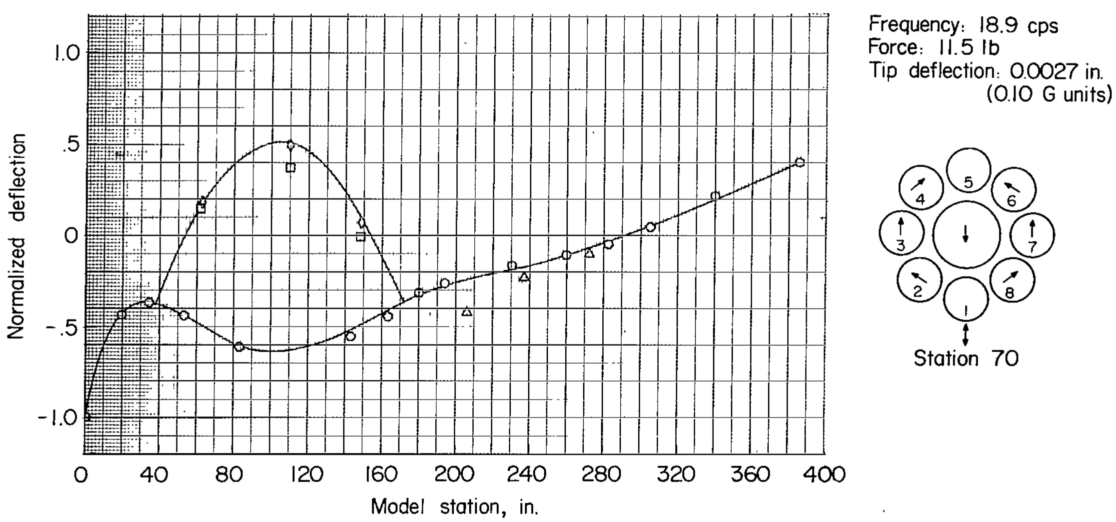

(f) Booster tank 100 percent full; link suspension.

Figure 11.- Concluded.

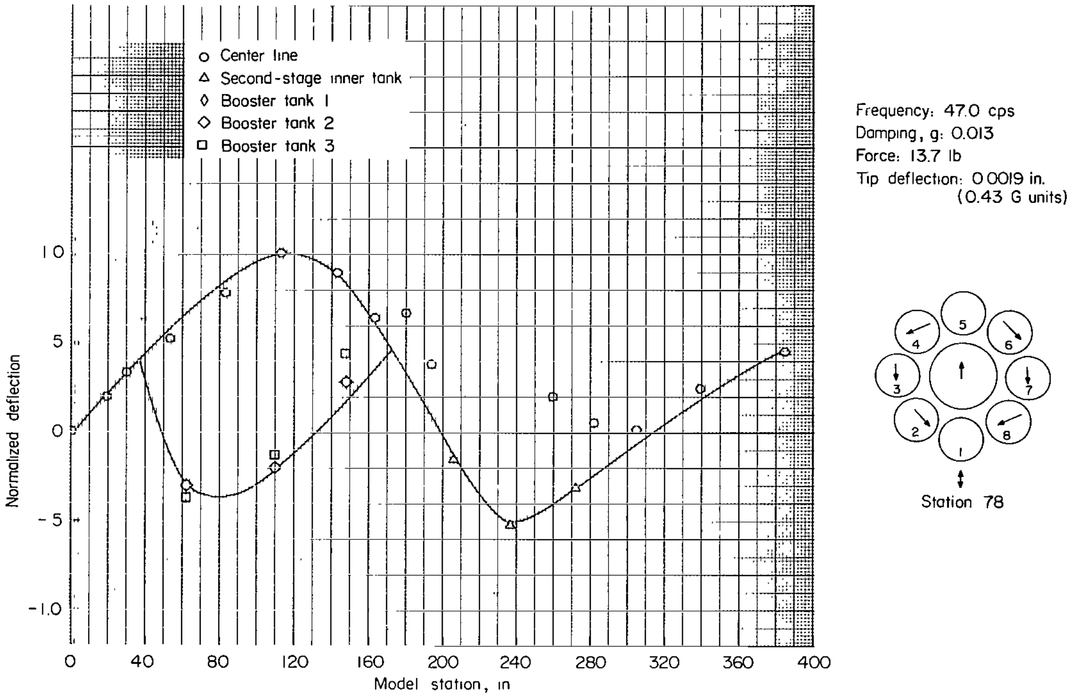

(a) Booster tank 25 percent full; spring suspension.

Figure 12.- Second cluster modes of 1/5-scale Saturn model.

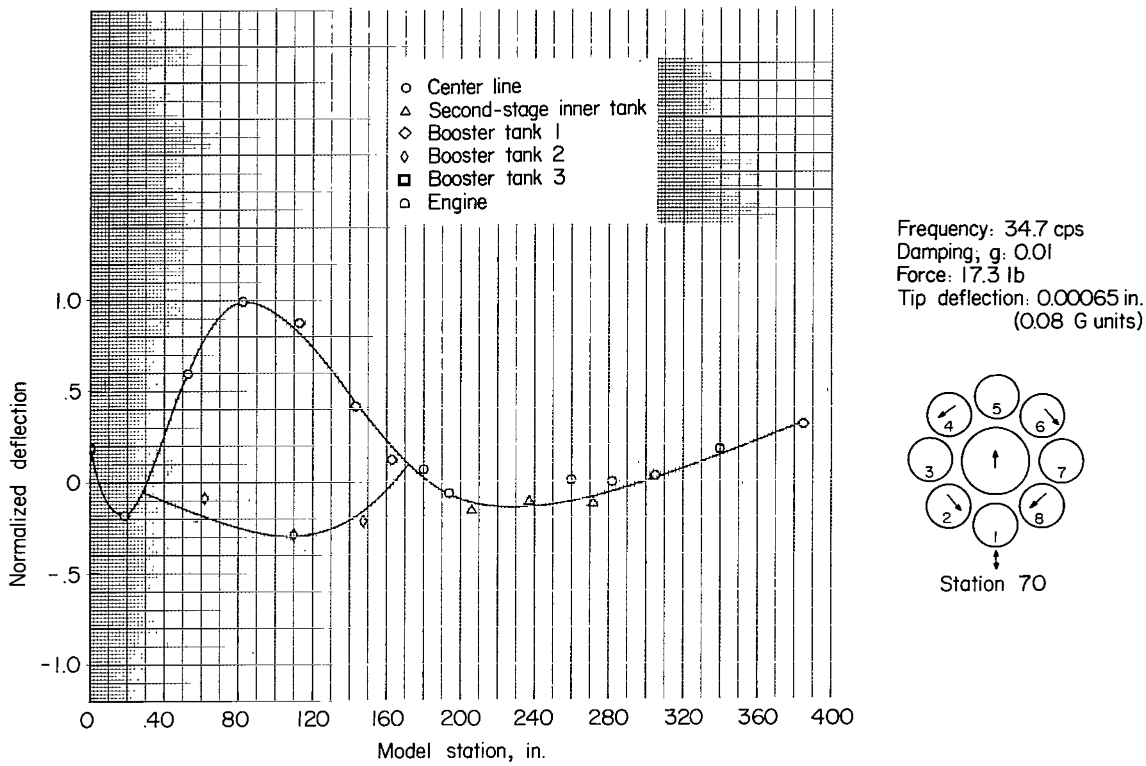

(b) Booster tank 48 percent full; spring suspension.

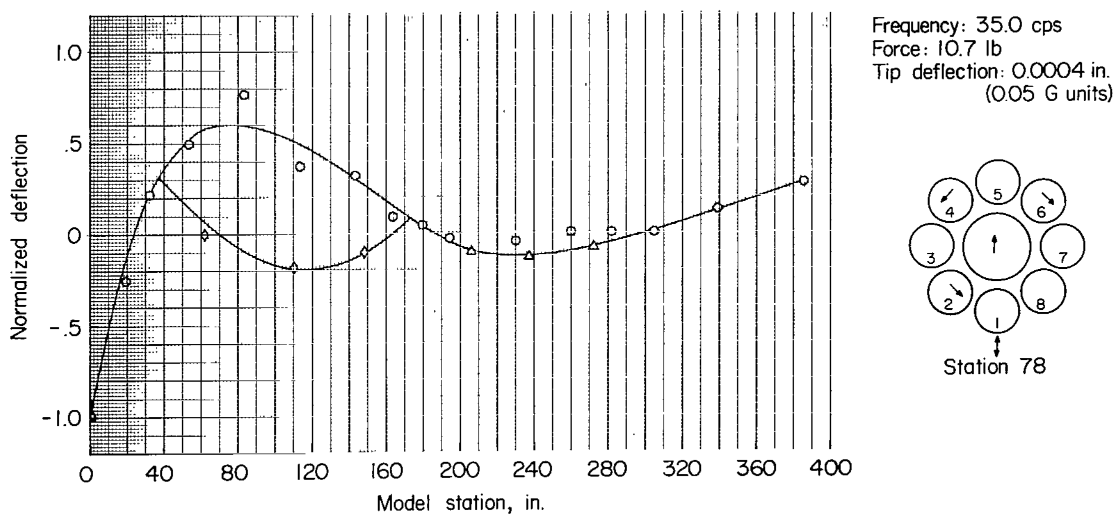

(c) Booster tank 48 percent full; link suspension.

Figure 12.- Continued.

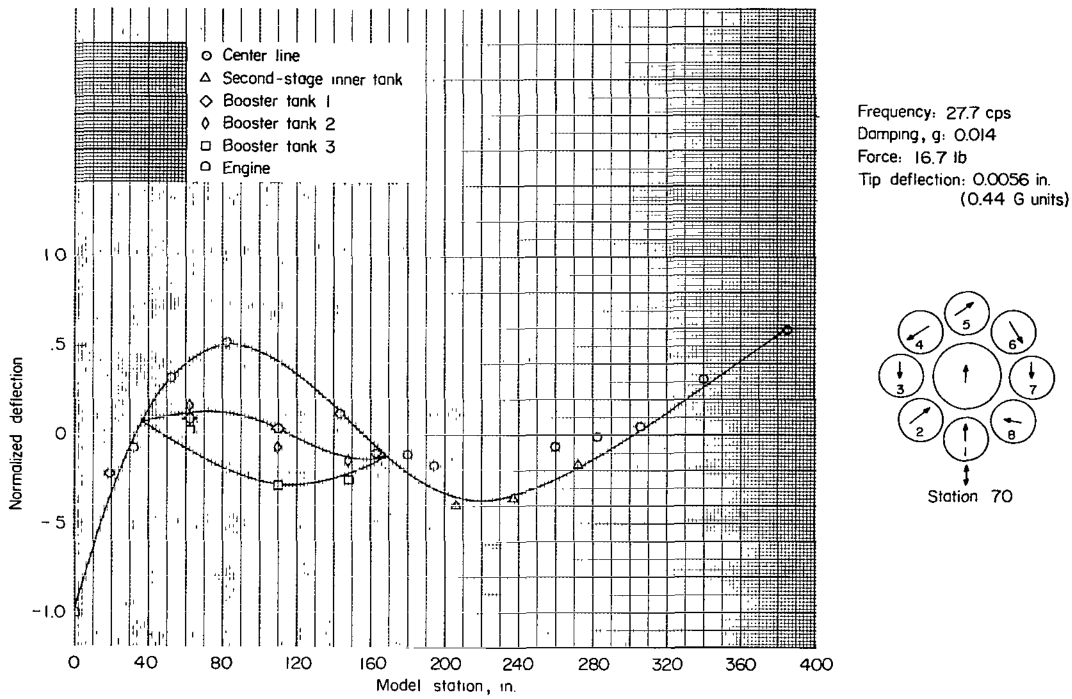

(d) Booster tank 75 percent full; spring suspension.

Figure 12.- Continued.

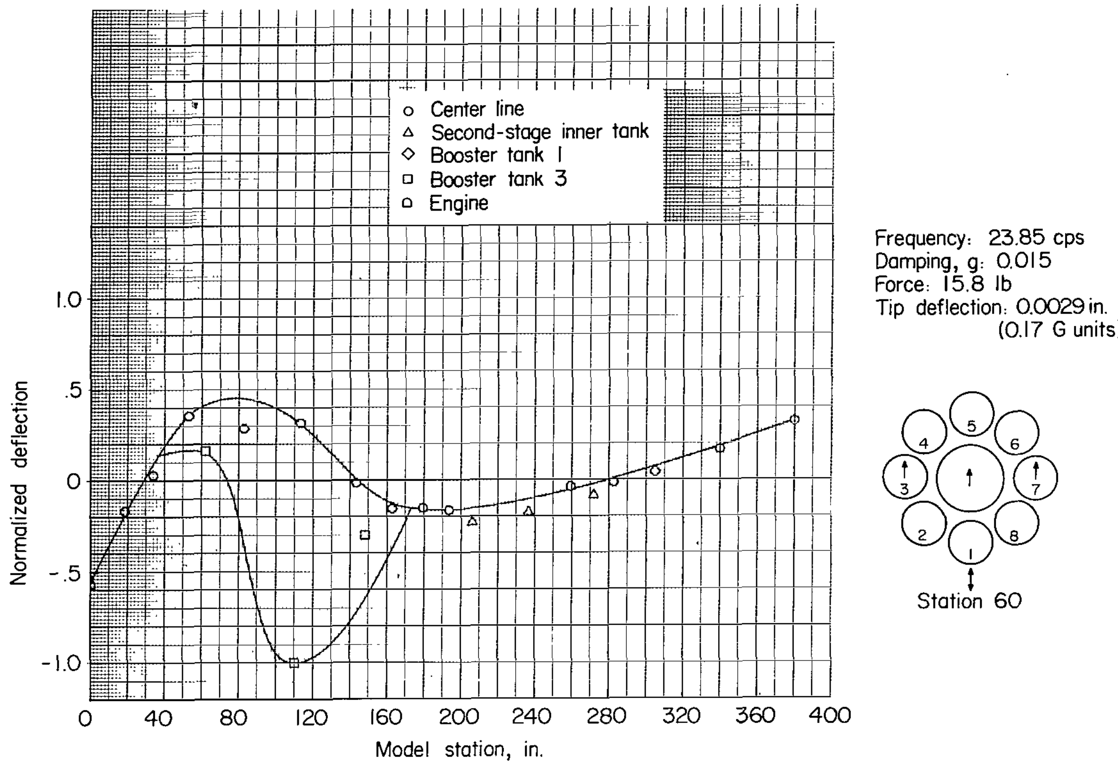

(e) Booster tank 100 percent full; spring suspension.

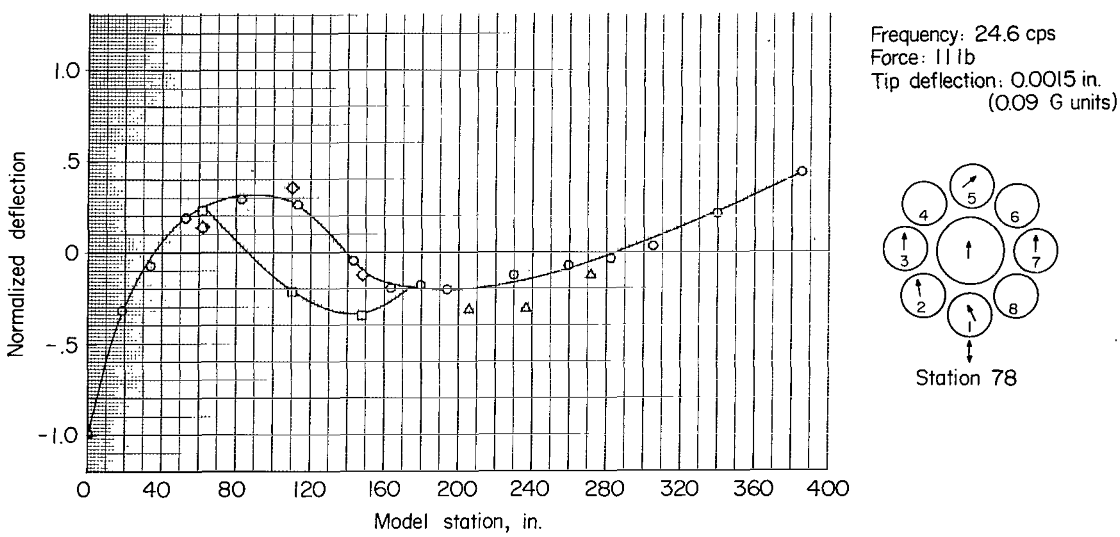

(f) Booster tank 100 percent full; link suspension.

Figure 12.- Concluded.

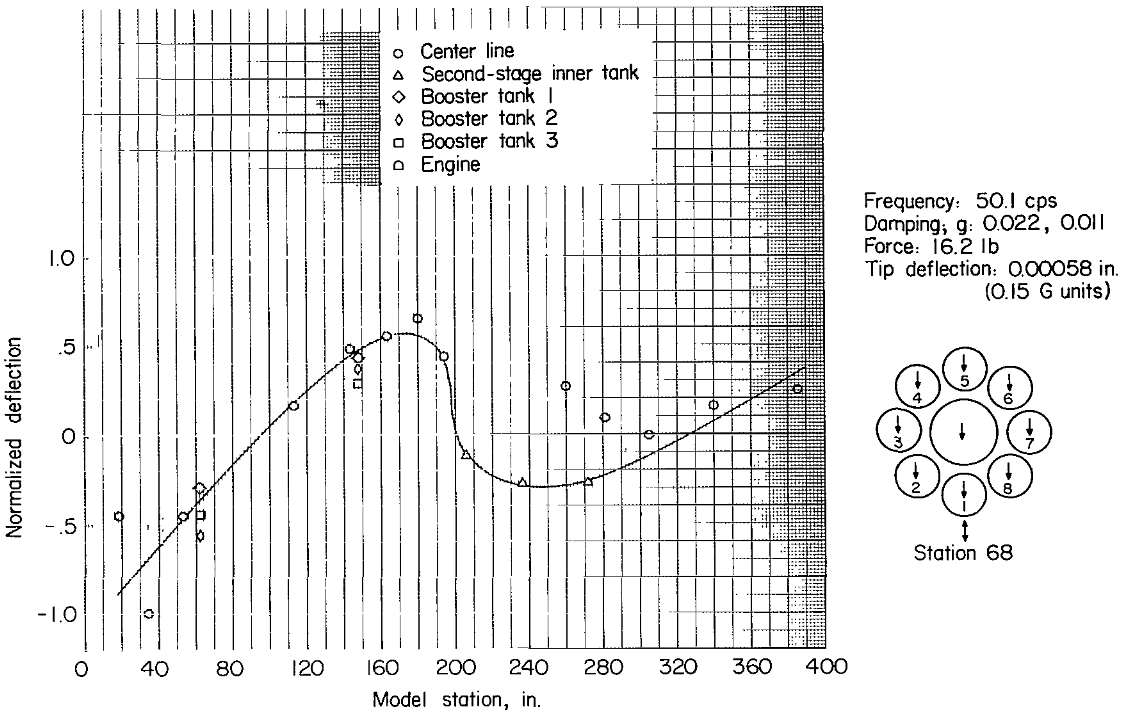

(a) Booster tank empty; spring suspension.

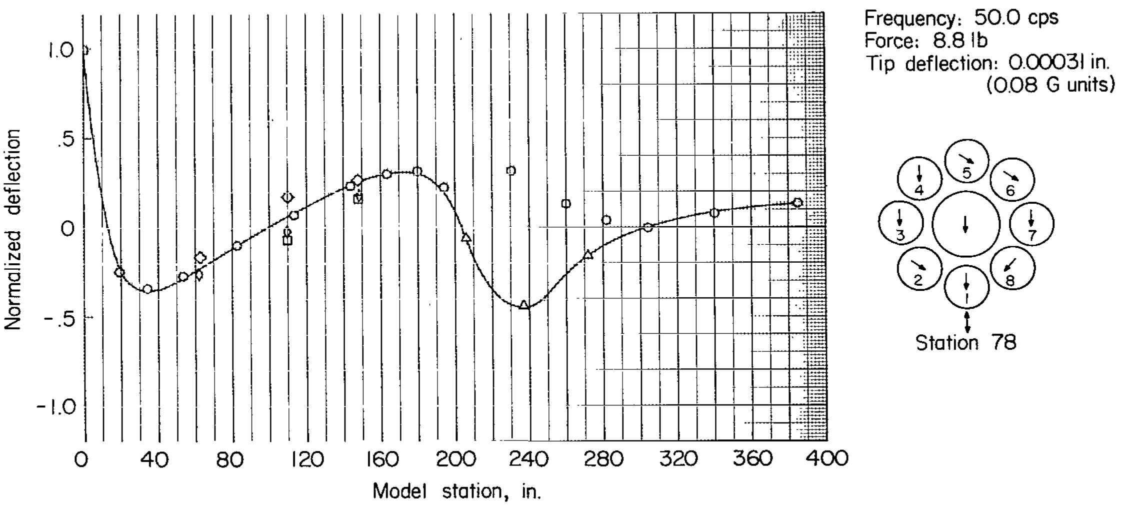

(b) Booster tank empty; link suspension.

Figure 13.- Second bending mode of 1/5-scale Saturn model. Group 1.

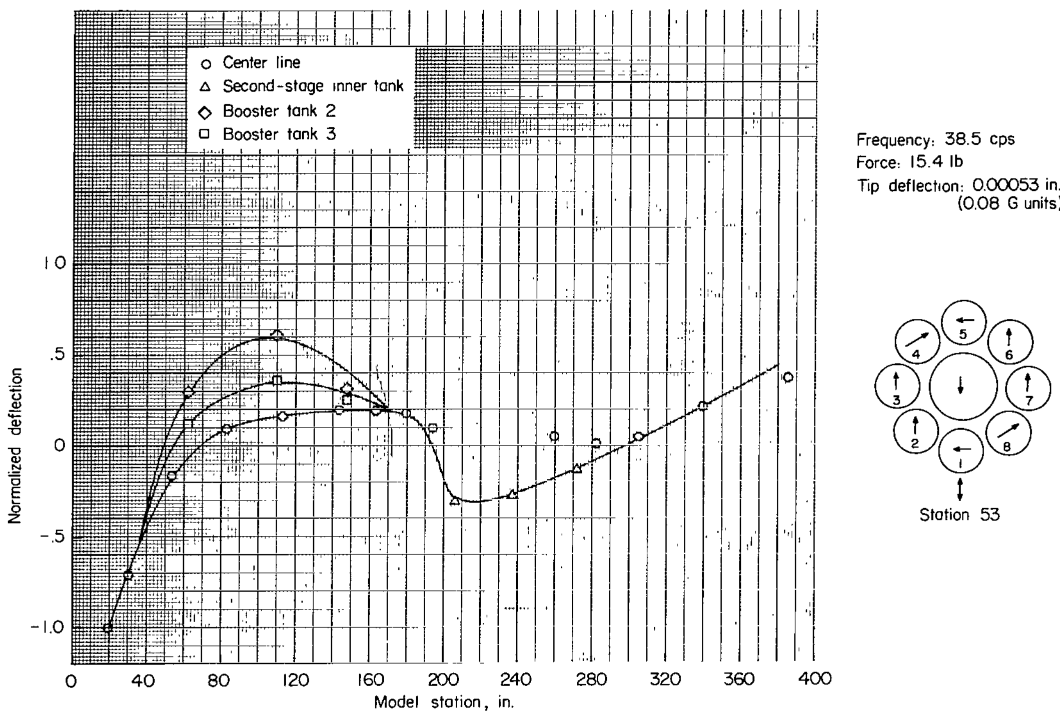

(c) Booster tank 25 percent full; spring suspension.

Figure 13.- Continued.

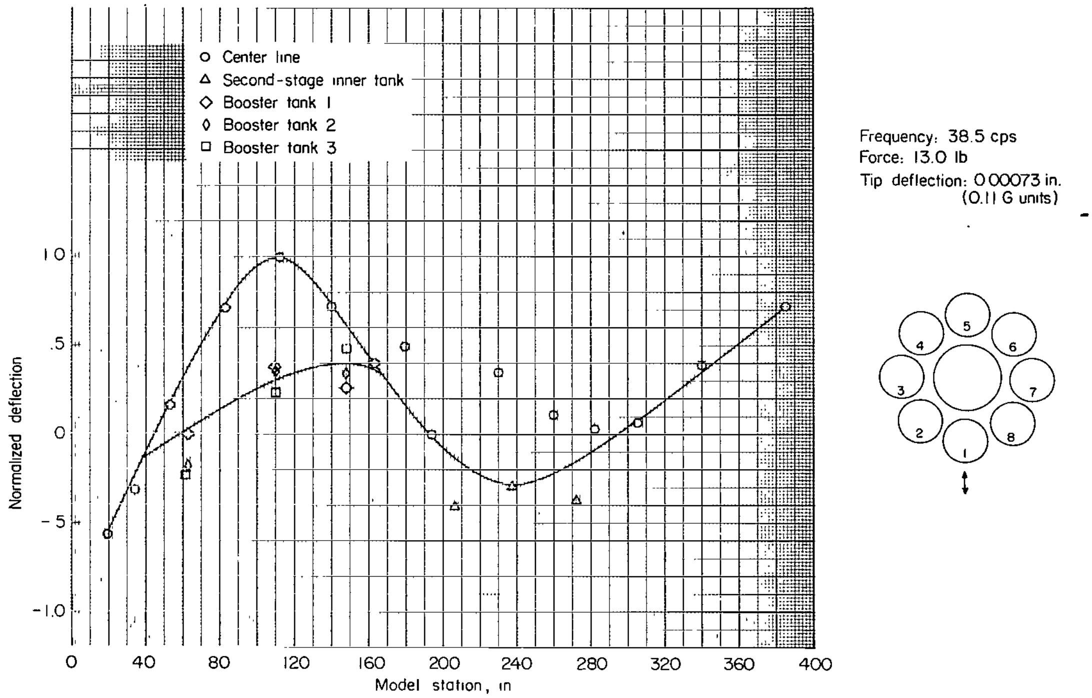

(d) Booster tank 48 percent full; link suspension.

Figure 13.- Continued.

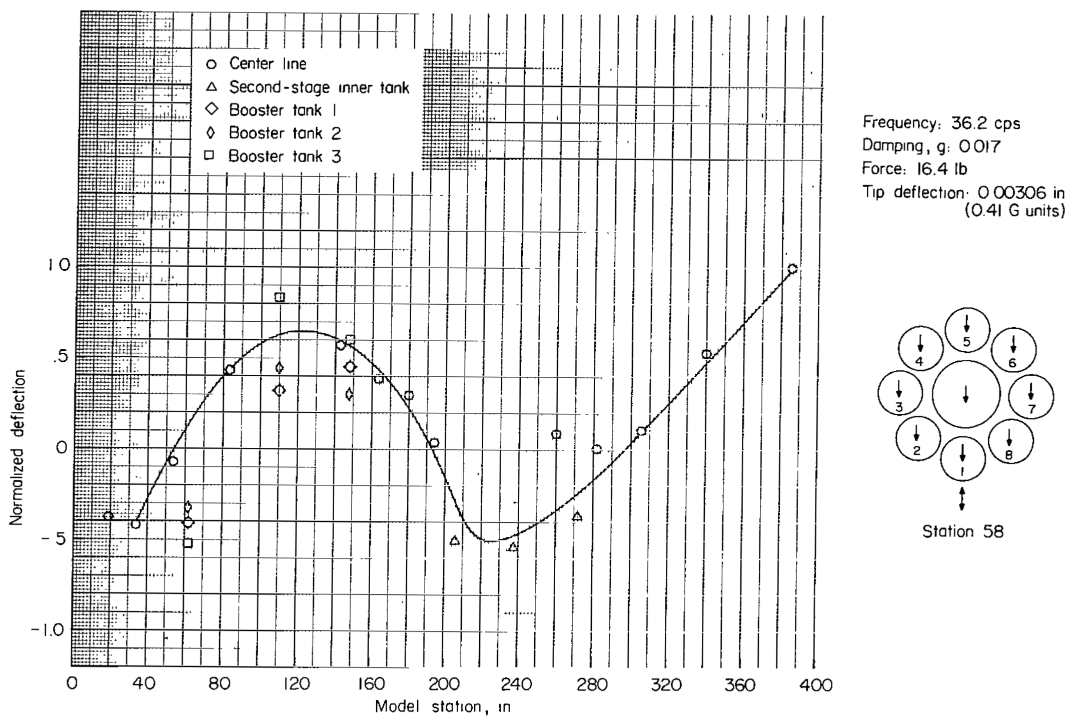

(e) Booster tank 75 percent full; spring suspension.

Figure 13.- Continued.

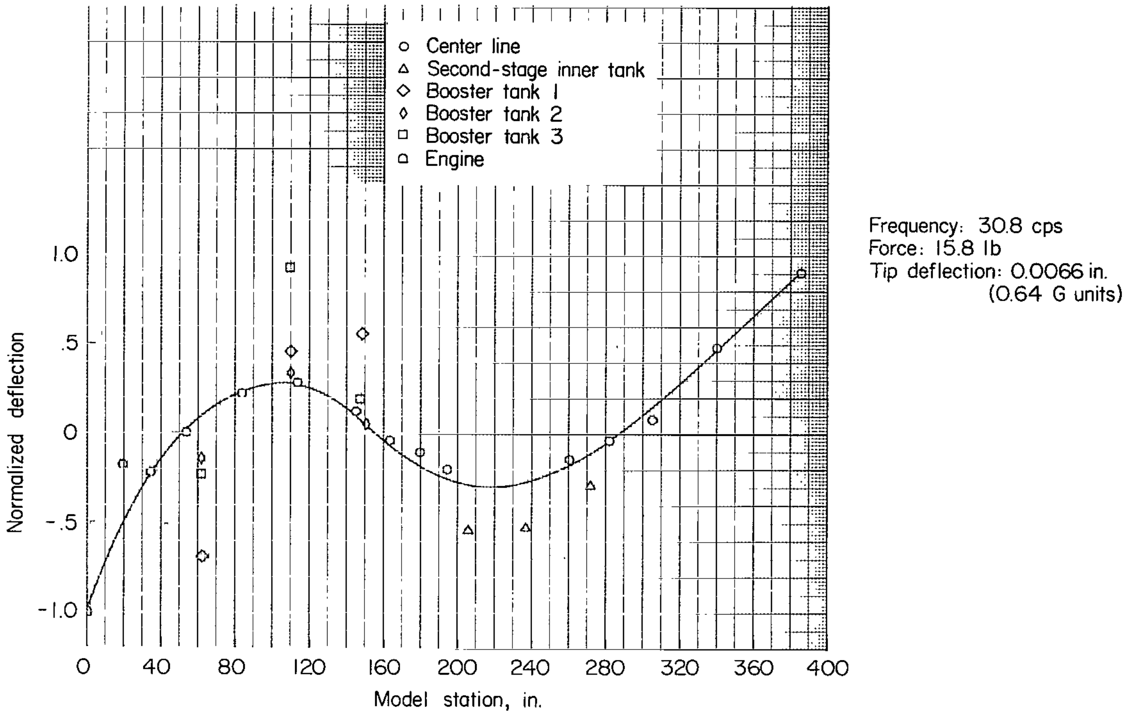

(f) Booster tank 100 percent full; spring suspension.

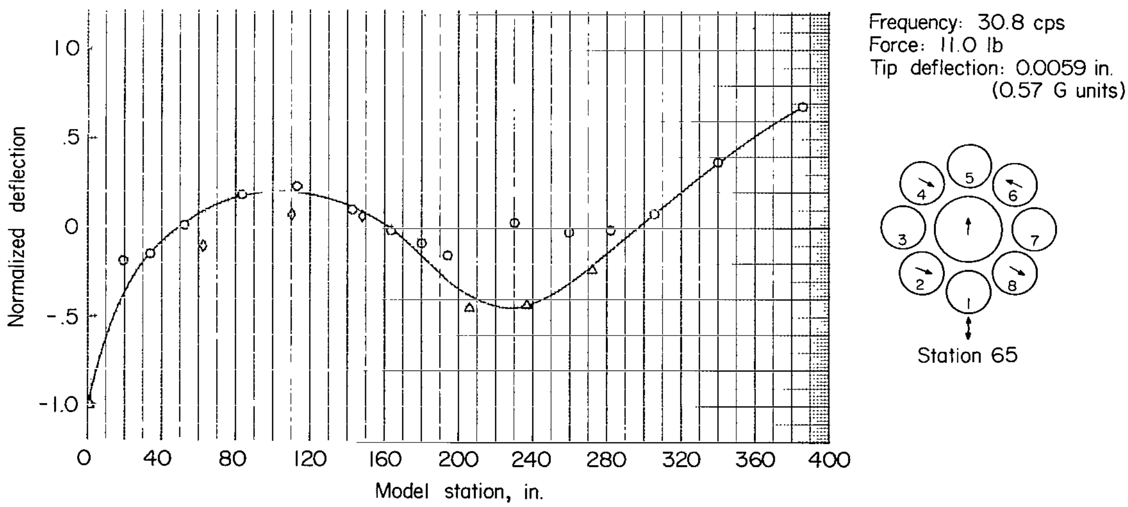

(g) Booster tank 100 percent full; link suspension.

Figure 13.- Concluded.

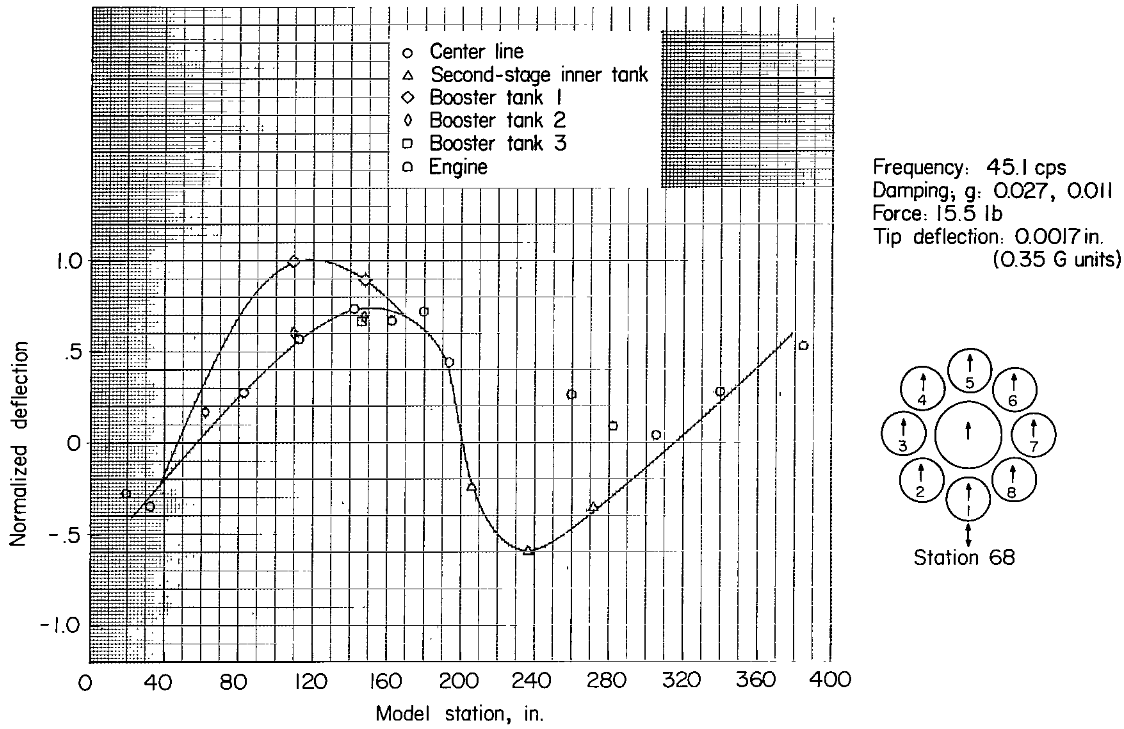

(a) Booster tank empty; spring suspension.

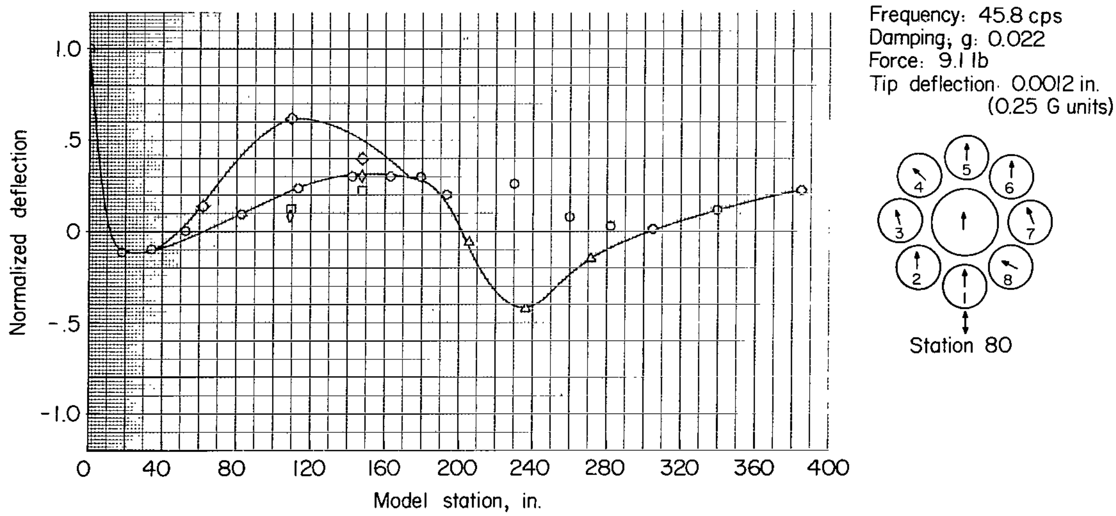

(b) Booster tank empty; link suspension.

Figure 14.- Second bending mode of 1/5-scale Saturn model. Group 2.

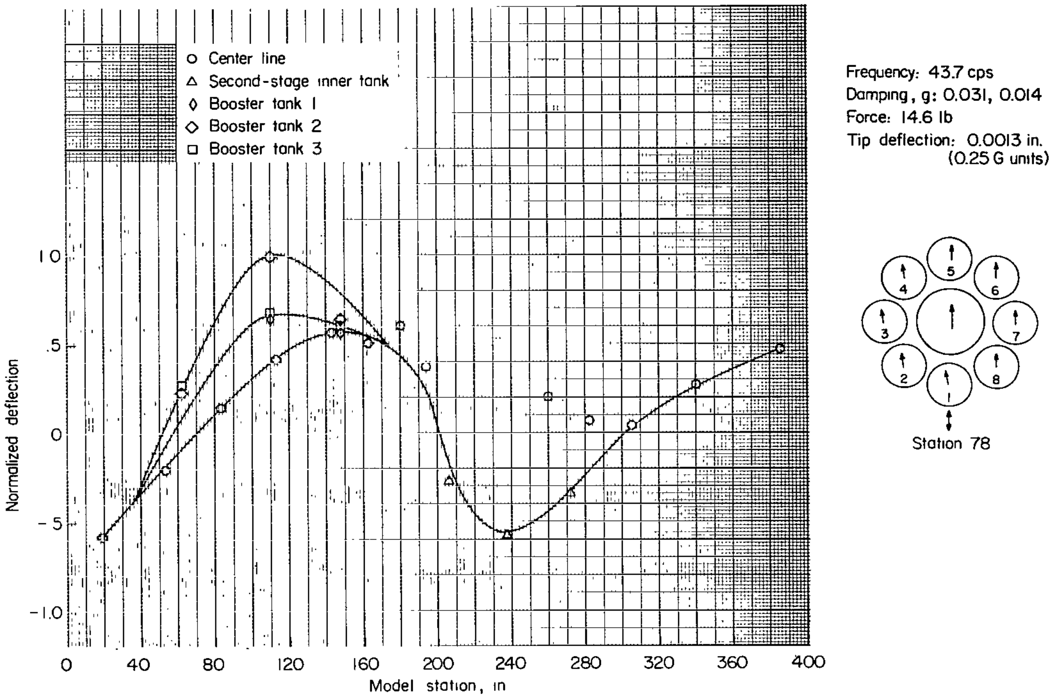

(c) Booster tank 25 percent full; spring suspension.

Figure 14.- Continued.

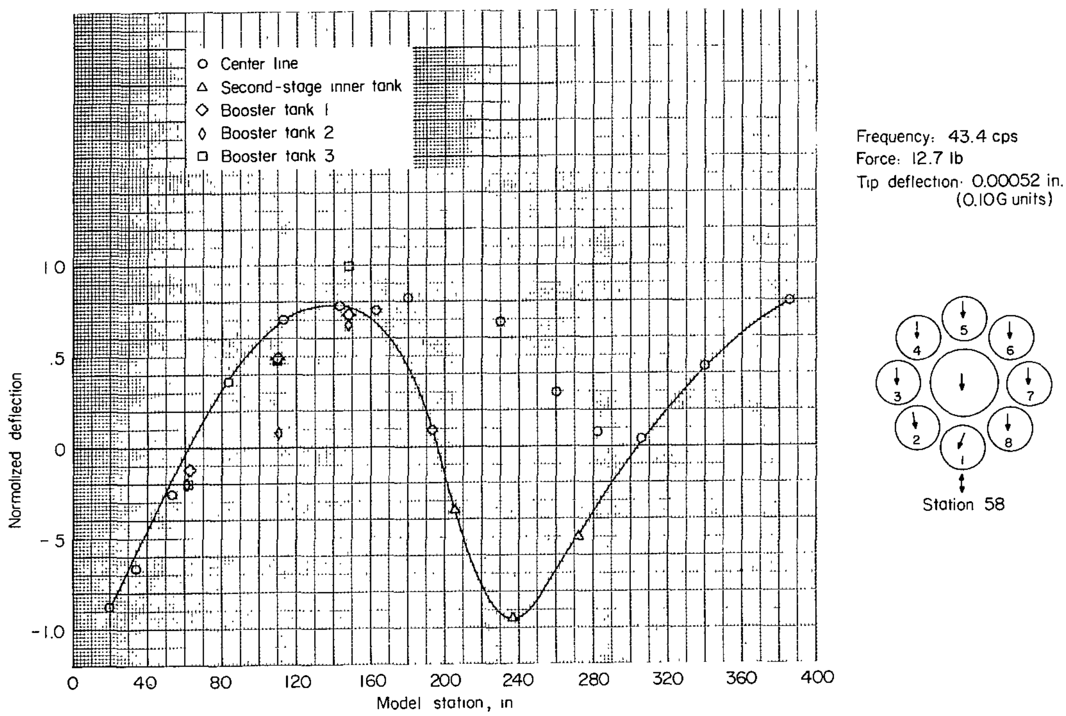

(d) Booster tank 48 percent full; link suspension.

Figure 14.- Concluded.

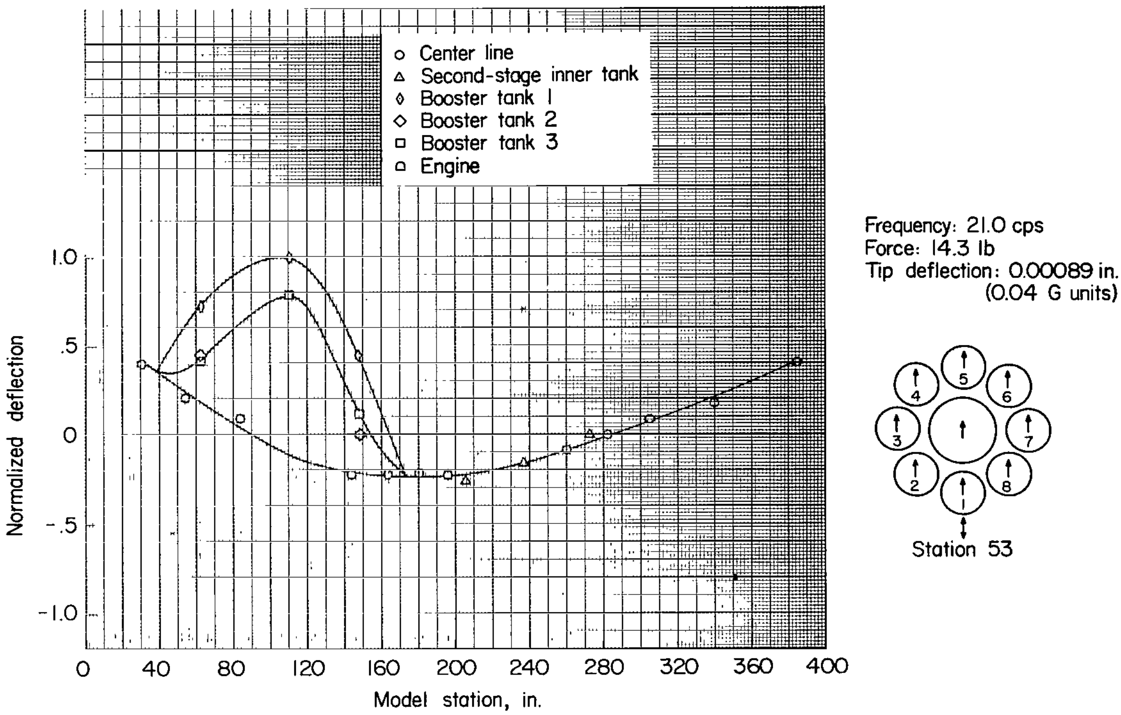

(a) Booster tank 25 percent full; spring suspension; outer tank coupled with first bending.

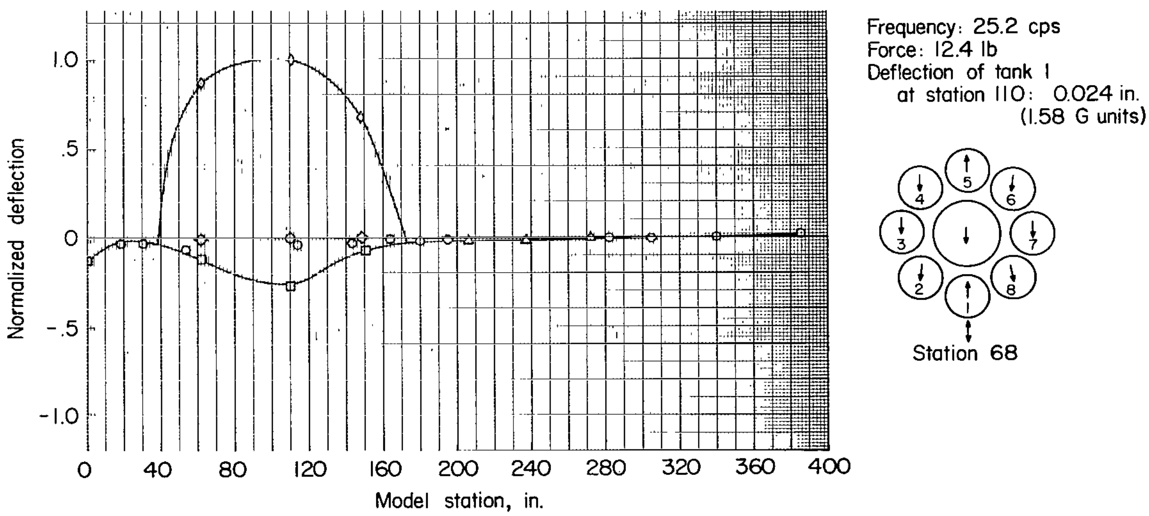

(b) Booster tank 25 percent full; spring suspension; outer tank only.

Figure 15.- Outer-tank modes of 1/5-scale Saturn model.

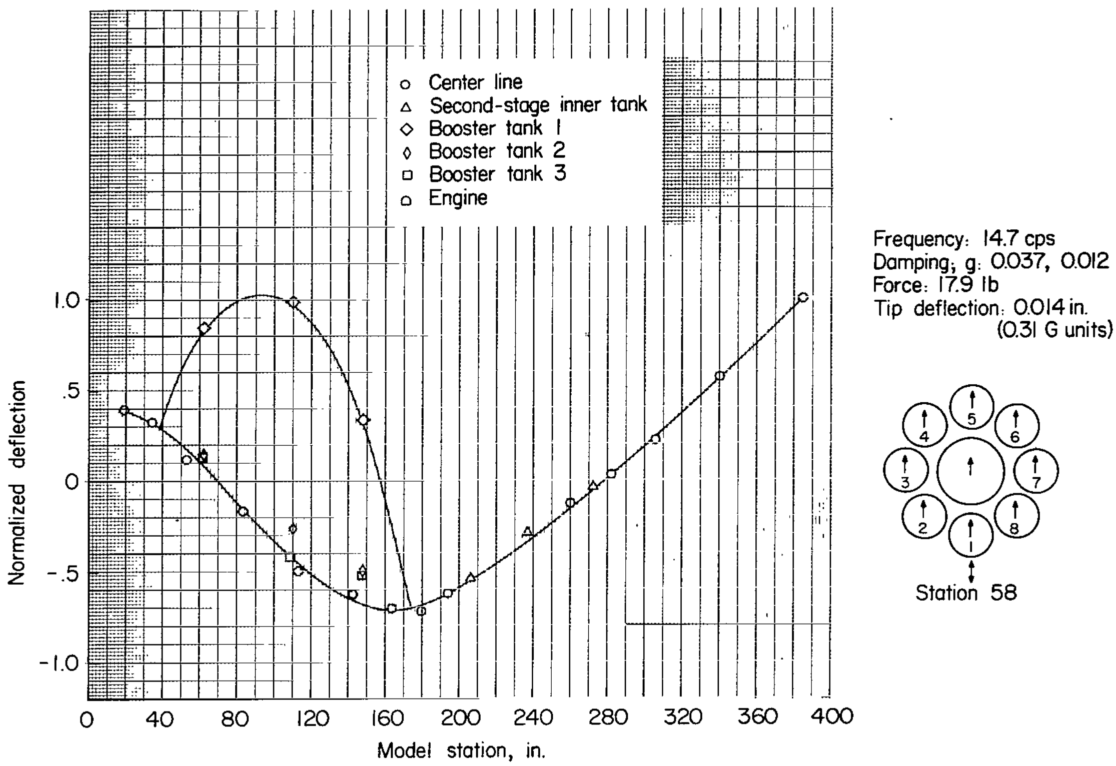

(c) Booster tank 48 percent full; outer tank coupled with first bending; spring suspension.

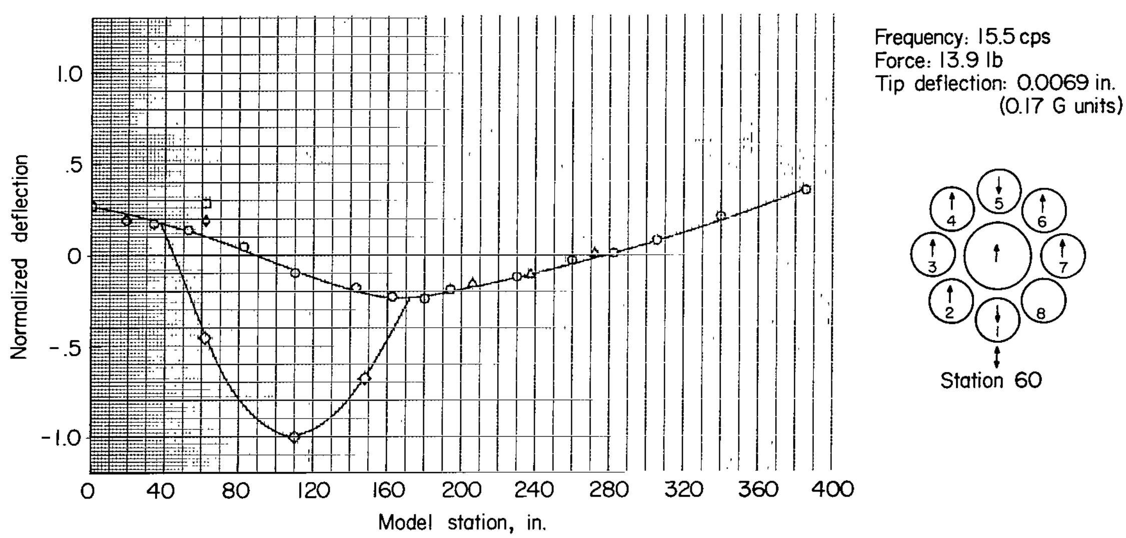

(d) Booster tank 48 percent full; outer tank coupled with first bending; link suspension.

Figure 15.- Continued.

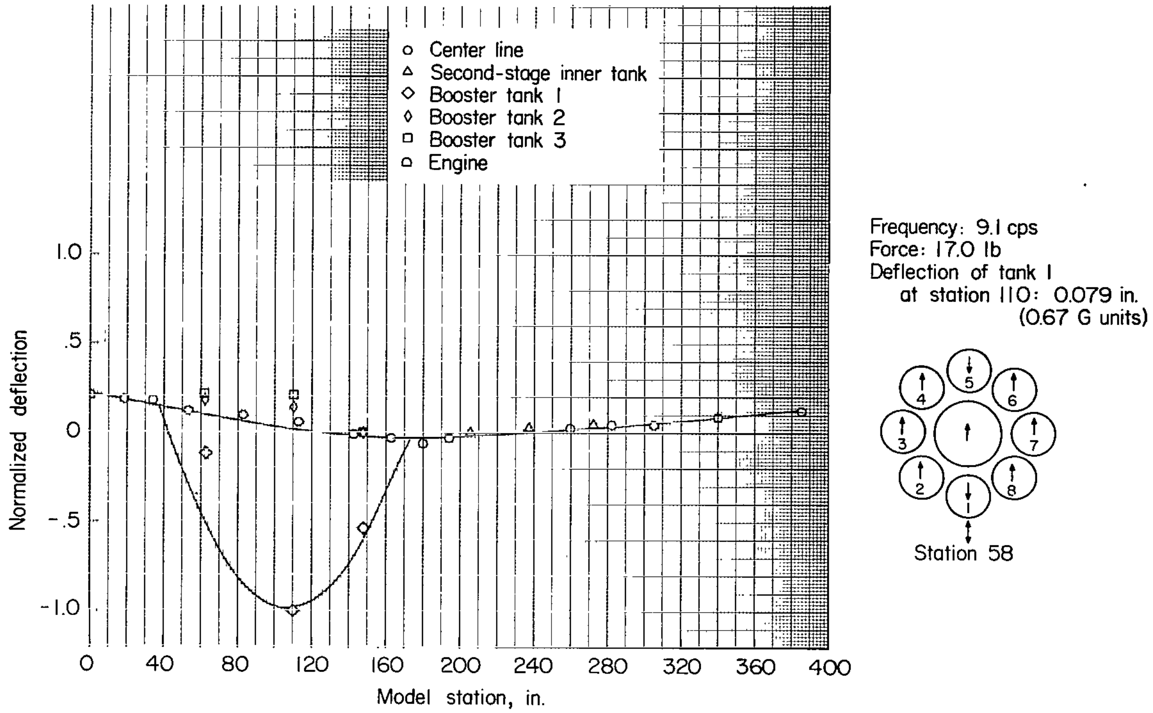

(e) Booster tank full; first bending of tank 1; spring suspension.

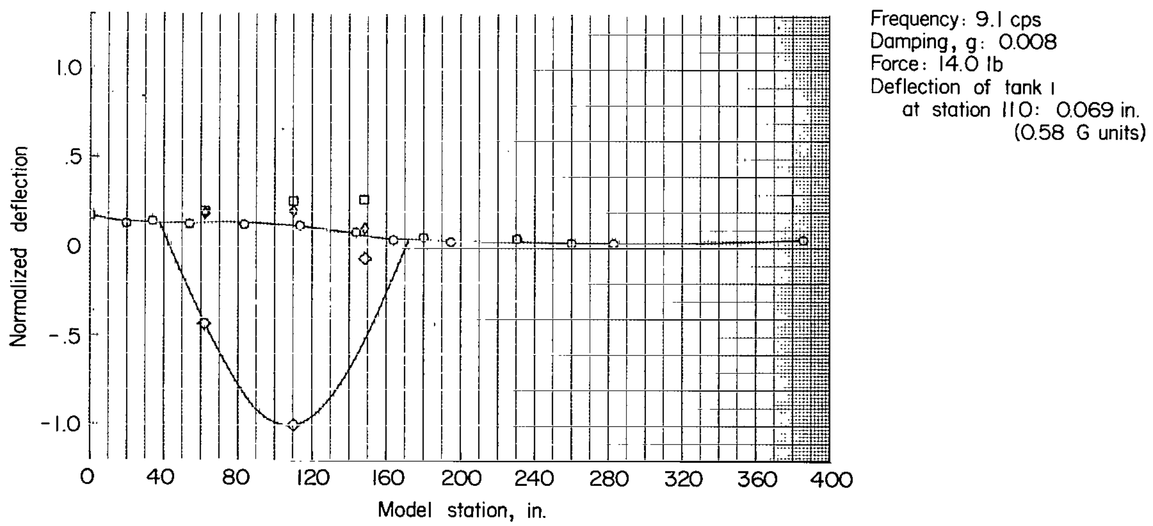

(f) Booster tank full; first bending of tank 1; link suspension.

Figure 15.- Concluded.

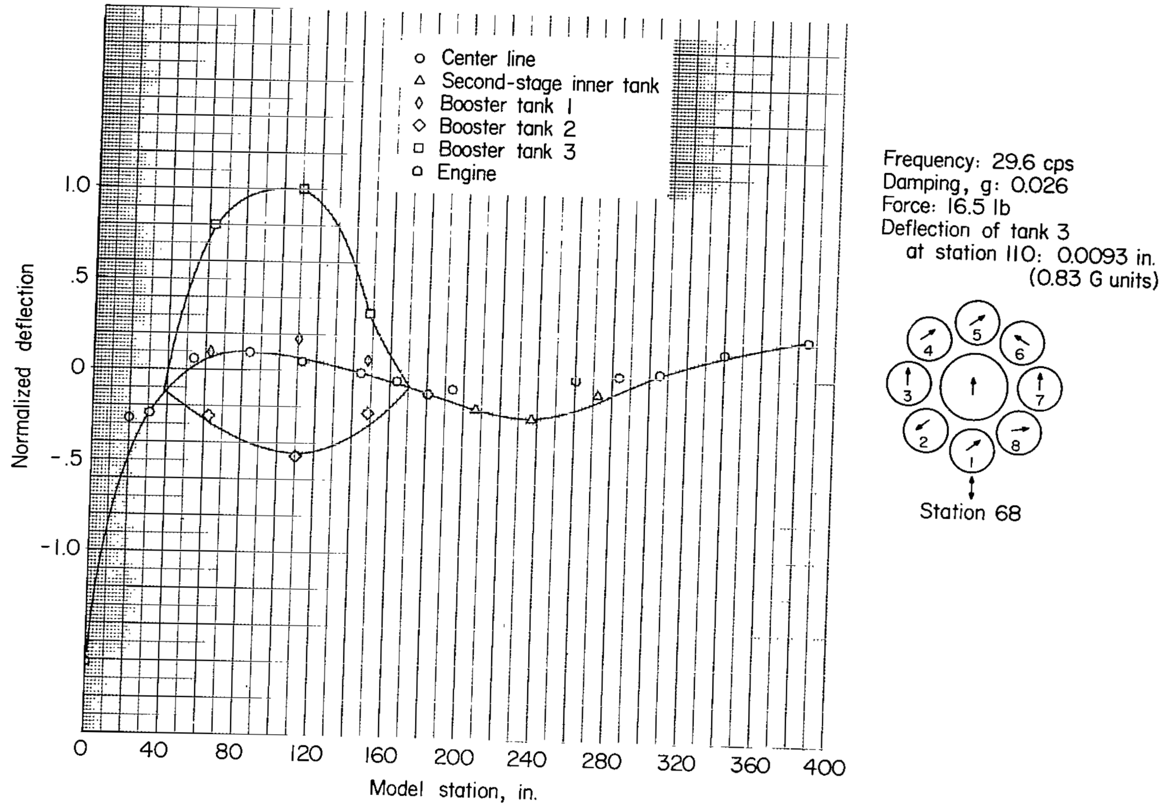

(a) Booster tank 25 percent full; spring suspension; center-line second bending and outer-tank first bending.

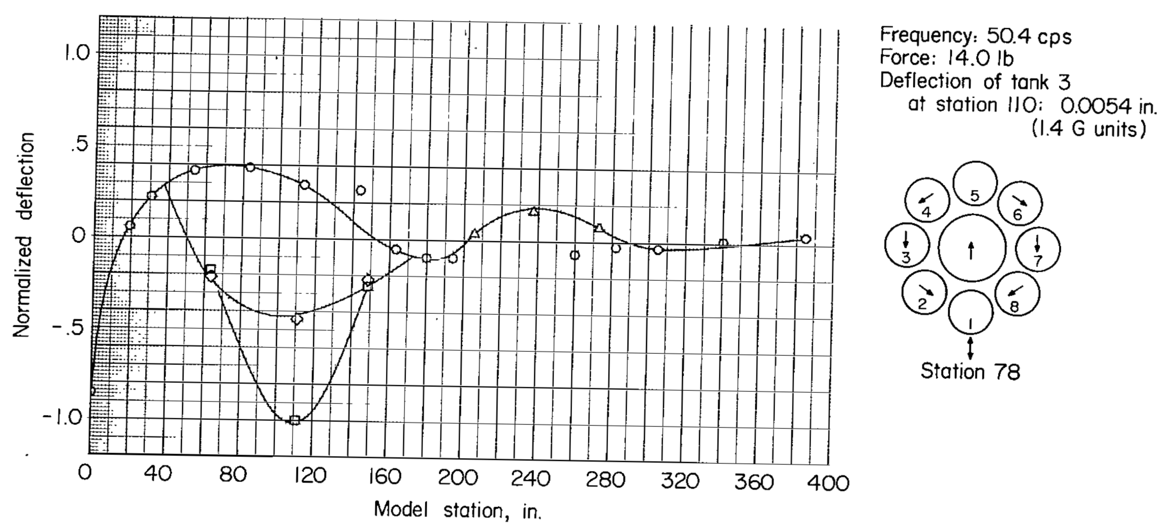

(b) Booster tank 25 percent full; spring suspension; third cluster mode.

Figure 16.- Miscellaneous modes.

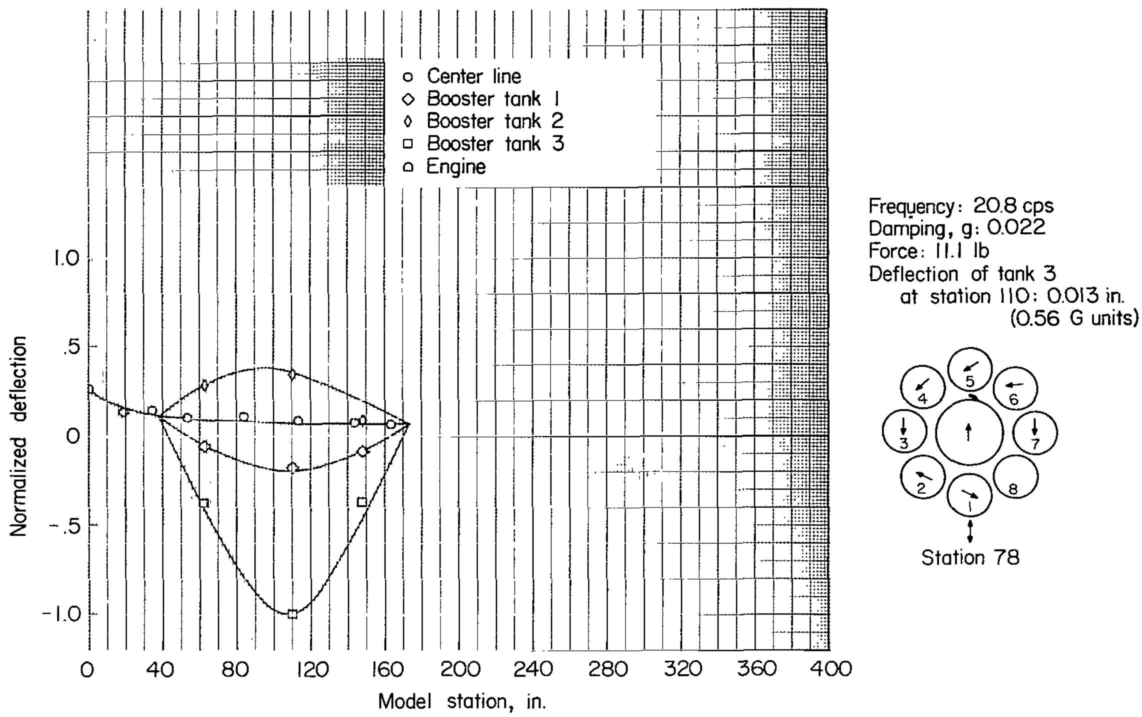

(c) Booster tank 48 percent full; booster mode; spring suspension.

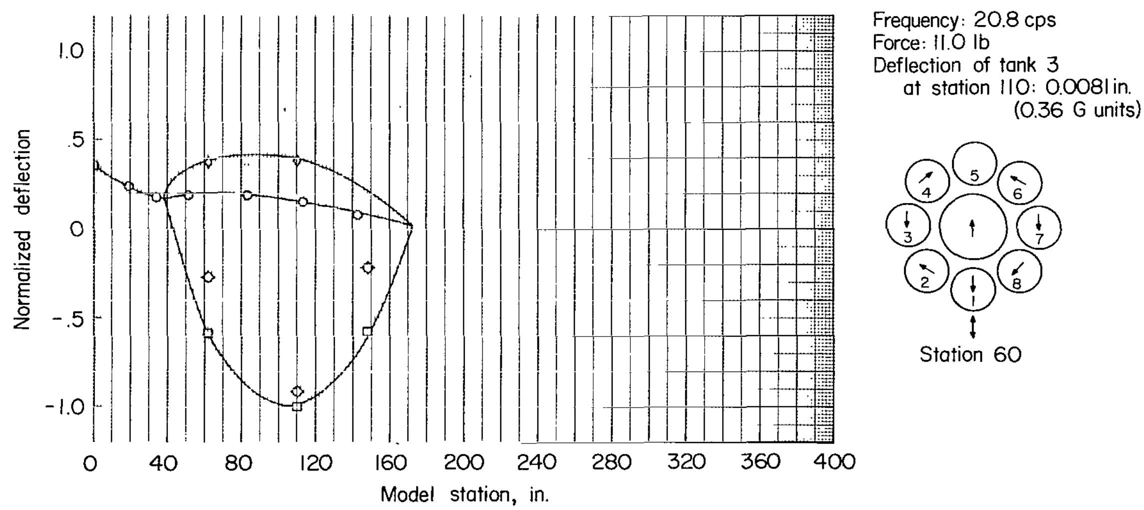

(d) Booster tank 48 percent full; booster mode; link suspension.

Figure 16.- Continued.

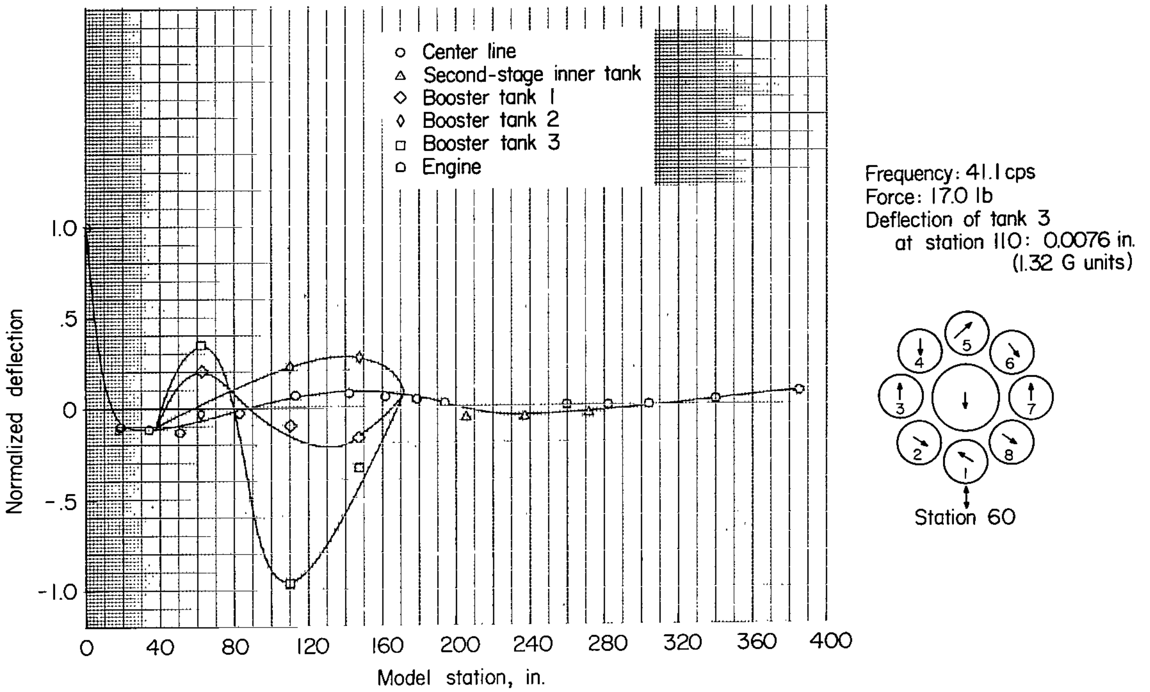

(e) Booster tank full; outer-tank second bending mode; spring suspension.

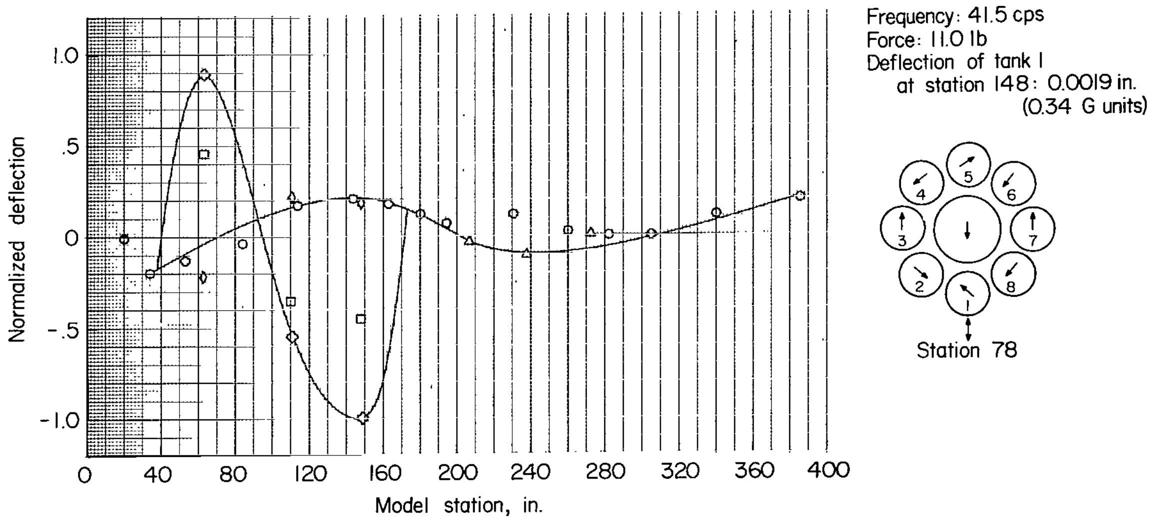

(f) Booster tank full; outer-tank second bending mode; link suspension.

Figure 16.- Continued.

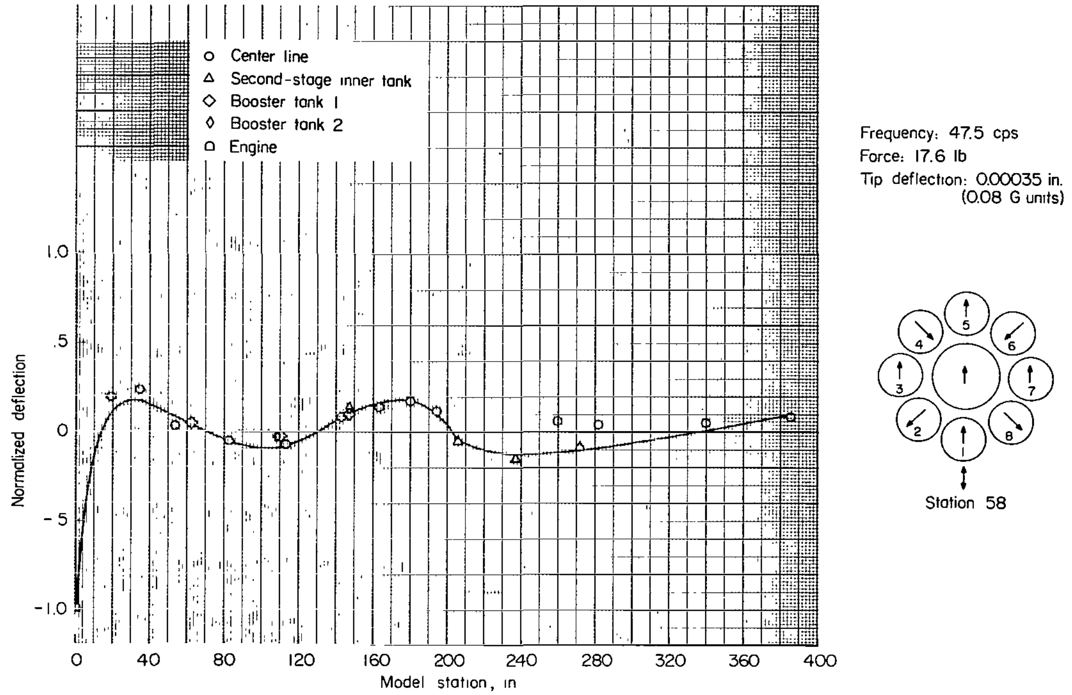

(g) Booster full, spring suspension, third bending mode.

Figure 16.- Concluded.

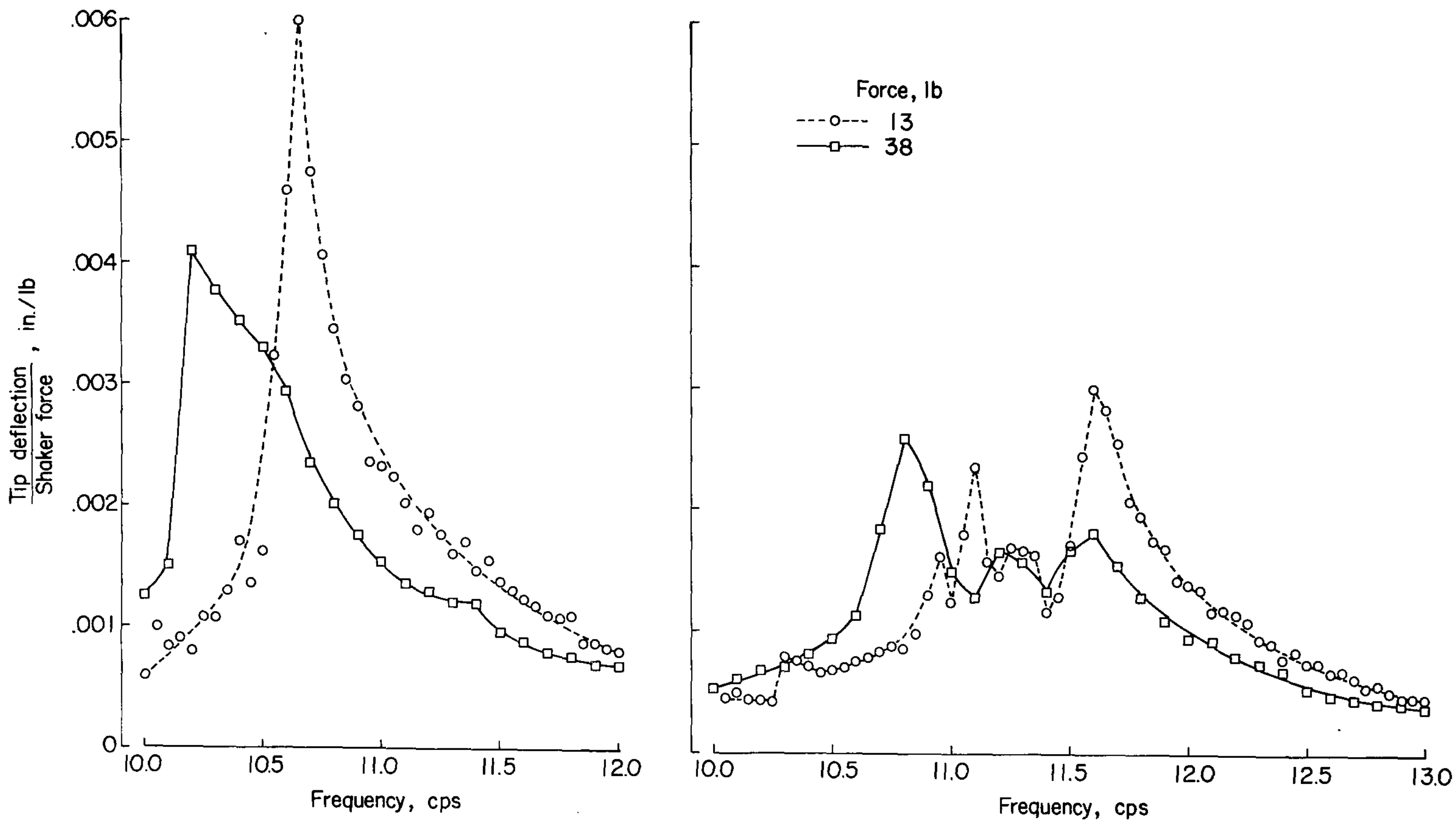

(a) Eight-cable spring suspension.

(b) Eight-cable link suspension.

Figure 17.- Frequency response of Saturn model.

NASA-Langley, 1964 L-3462

2/7/85

"The aeronautical and space activities of the United States shall be conducted so as to contribute . . . to the expansion of human knowledge of phenomena in the atmosphere and space. The Administration shall provide for the widest practicable and appropriate dissemination of information concerning its activities and the results thereof."

—NATIONAL AERONAUTICS AND SPACE ACT OF 1958

NASA SCIENTIFIC AND TECHNICAL PUBLICATIONS

TECHNICAL REPORTS: Scientific and technical information considered important, complete, and a lasting contribution to existing knowledge.

TECHNICAL NOTES: Information less broad in scope but nevertheless of importance as a contribution to existing knowledge.

TECHNICAL MEMORANDUMS: Information receiving limited distribution because of preliminary data, security classification, or other reasons.

CONTRACTOR REPORTS: Technical information generated in connection with a NASA contract or grant and released under NASA auspices.

TECHNICAL TRANSLATIONS: Information published in a foreign language considered to merit NASA distribution in English.

TECHNICAL REPRINTS: Information derived from NASA activities and initially published in the form of journal articles.

SPECIAL PUBLICATIONS: Information derived from or of value to NASA activities but not necessarily reporting the results of individual NASA-programmed scientific efforts. Publications include conference proceedings, monographs, data compilations, handbooks, sourcebooks, and special bibliographies.

Details on the availability of these publications may be obtained from:

SCIENTIFIC AND TECHNICAL INFORMATION DIVISION

NATIONAL AERONAUTICS AND SPACE ADMINISTRATION

Washington, D.C. 20546